1980

Some aspects of the reactor design for bulk polymerization of vinyl chloride.

Jorge Nestor Farber
University of Massachusetts Amherst

SOME ASPECTS OF THE REACTOR DESIGN FOR BULK POLYMERIZATION OF VINYL CHLORIDE

A Thesis Presented

By

JORGE NESTOR FARBER

Submitted to the Graduate School of the
University of Massachusetts in partial fulfillment
of the requirements for the degree of

MASTER OF SCIENCE

September 1980

Polymer Science and Engineering Department

SOME ASPECTS OF THE REACTOR DESIGN FOR BULK POLYMERIZATION OF VINYL CHLORIDE

A Thesis Presented

By

JORGE NESTOR FARBER

Approved as to style and content by:

Dr. Robert L. Laurence, Chairperson of Committee

Dr. Richard J. Farris, Member

Dr. James C. W. Chien, Member

Dr. William J. MacKnight,
Department Head
Polymer Science and Engineering
Department

TABLE OF CONTENTS

LIST OF FIGURES

CHAPTER I

INTRODUCTION

The bulk polymerization of vinyl chloride is still at the present time far from being well understood. In spite of the economic importance of the process, the detailed quantitative behavior of the reactor has not been elucidated. Immediate reasons for this, are given by the physical complexities of particle formation (arising from oligomer precipitation in solution), and heterogeneous polymerization kinetics, recalling that the process starts with one liquid monomer phase and finishes with three phases: liquid and gaseous monomer, and solid polymer.

Among the different contributions to a better comprehension of the problem, it is easy to discover a lack of uniform criteria, not only in the strictly chemical aspect of the problem (i.e., well defined kinetic steps), but also in the complicated physical phenomena inherent to the heterogeneous multiphase reacting system. In addition to this, we should mention another kind of difficulties originated not in the understanding of the process, but in its description: i.e., mathematical complexity in formulating and solving the multivariate distributions of particle properties, that cannot be obviated for the purpose of a quantitative useful mode.

The emphasis of this work will be in the description of a detailed mathematical model for a bulk polymerization reactor, which will require:

a) development of a detailed kinetic model, efficient in performing the normally observed behavior like acceleration, dependence with initiator and chain transfer agent concentration, monomer-polymer equilibrium, etc.

b) The formulation of an agglomeration model capable to predict the particle size distribution.

c) To attempt a numerical solution of the kinetic equation and the four population balances that describe different particle properties, and necessary to predict particle size and molecular weight distributions.

d) Based on the available kinetic and thermodynamic data, to search for optimal reactor conditions, i.e., given a specified property in the final product like its molecular weight, to program the optimal temperature and reaction time.

C H A P T E R I I

LITERATURE REVIEW

2.1 The Physical Picture

Bulk polymerization is the oldest and the simplest process for the polymerization of monomer substances. Its importance is not limited to the preparation and study of high polymers in the laboratory but also applies to industrial mass polymerization processes. Some of its advantages are:

a) the use of simple equipment and lower amount of investment as there is neither water nor solvent to be separated;

b) rapid reactions and a good yield;

c) polymers have high purity, with good stability and excellent transparency;

d) the "bulk" PVC granules exhibit higher porosity than the ones obtained by suspension or emulsion polymerization. The different morphology originates in different association mechanisms, recalling that bulk polymerization is normally effected in the absence of emulsifiers or protective colloids.

On the other hand, bulk polymerization generally involves two difficulties:

- One concerns the agitation of the medium. This is especially true when the polymer is soluble in the monomer since the viscosity increases considerably as the reaction proceeds.
- The other concerns the elimination of the heat given off in the course of the polymerization reaction. For the polymerization of the poly-addition type, the propagation of the chains which results from the transformation of a double bond into two simple bonds is a very exothermic reaction. Heat transmission by conduction and convection is difficult when the viscosity of the medium is high, or when there is present a polymer insoluble in its monomer. The heat transfer coefficient between a powdered solid and the wall of a reactor is poor.

To overcome these two difficulties, the process of polymerization in suspension was developed even though it presented other major inconveniences. The dispersions of solid granules in water are easy to agitate, and the water serves as a thermal capacitance allowing significant increase in the total heat transfer coefficient.

Advantages of bulk polymerization in systems with low monomer polymer compatibility

Vinyl chloride is a liquid which boils at -14°C and has a very low viscosity (0.2 cp at -14°C, 0.193 cp at 25°C). The polymer is insoluble in the monomer and precipitates to form beads which even under a slight agitation do not have a tendency to agglomerate.

The medium can be agitated in a homogeneous way without difficulty. The temperature of polymerization is generally between 40°C and 70°C, and the monomer in the reactor is under a pressure from 5 to 12 Kg/cm^2 (75-175 psi).

The liquid monomer is constantly in equilibrium with its vapor, and it is easy to remove the heat of reaction by distillation and recondensation of the monomer on the wall of the reactor or in a reflux heat exchanger. In the same way, the unreacted vinyl chloride monomer may be removed at the end of the reaction. This condition produces a particularly favorable situation when polymerizing vinyl chloride in bulk.

One step bulk polymerization

One step polymerization is a reaction which is carried out entirely in the same reactor. On the other hand, a two step polymerization is successively realized in two reactors of different types (1), (2).

The one step polymerization is the most generally used process for bulk polymerization. This technique has been used by all those who have tried to achieve the bulk polymerization of vinyl chloride, in laboratory as well as in industrial scale. In all cases conventional apparatus has been used, and it is here that the essential cause of failure arises. This type of reaction presents the following peculiarities:

- It begins in an homogeneous liquid medium of very low viscosity.

- It ends in an essentially solid phase, the vinyl chloride monomer being absorbed by the PVC beads.
- The volume occupied by the medium doubles from the beginning to the end of the polymerization.

The major difficulties revealed are:

- In case of a bad agitation of the solid phase, the eventuality of coagulation and afterward the possibility of an uncontrollable reaction.
- In case of a badly adapted agitation in the liquid phase the production of a polymer of low apparent density and of large particle size distribution.

For several years a one step polymerization process was successfully exploited by Pechiney-Saint Gobain. The resins produced answered the criterium of purity (heat stability and transparency) hoped for in bulk resins. One of their applications was in the field of artificial yarns, where they gave results superior to suspension resins and even more so to emulsion resins. Nevertheless the limitation in the use of these resins was due to their low apparent density and to their large particle size distribution that did not allow for their use in the new techniques of transformation directly from powder.

Two step bulk polymerization

The principal objections to the bulk polymerization process of vinyl chloride are of two types:

- Technological: There are difficulties in conducting a reaction which begins in a liquid medium of 0.9 density in order to end in a powdery medium with a bulk density of 0.5.
- Structural: The resins obtained have more often a larger particle size distribution and a low apparent density.

The reaction mechanism shows clearly that it is possible and desirable to realize the bulk polymerization of vinyl chloride in two steps.

The first step is carried out in an essentially liquid medium and is a bead formation phase. The step is short since these beads are formed as soon as 3% of vinyl chloride is polymerized; however, a rate of conversion of 7% is necessary for sufficient cohesion of the beads or particles.

The second step is a growing phase for the beads and can be accomplished in an apparatus suitable to the reactions in a powdery medium.

The initial phase, called prepolymerization, is realized in a stainless steel vertical autoclave (Figure 1).

The conditions of agitation have a dominant influence on the determination of the bead structure, and it was found that a very turbulent agitation is necessary in order to obtain spherical beads of high density.

It is also important to equip the prepolymerizer with a flat blade turbine and baffles to avoid the formation of a vortex in this

very low viscosity medium. The volume of the industrial reactors is about 8 cu. m.

Experiments showed that it is not necessary to prepolymerize the total batch of vinyl chloride monomer. Prepolymerization of half the batch is sufficient to suitably seed the reaction and to obtain a resin of satisfying structure in the second reactor. This allows for the size of the prepolymerizer to be cut in half.

Control of particle structure

The essential phase of the reaction in the determination of the particle structure is in the prepolymerization phase. According to the nature of the agitation, either regular spherical beads or beads without any geometrical form, whose particle size distribution is large, are obtained. The average dimension of the beads varies with the intensity of the turbulent agitation.

In modifying the intensity of the agitation, it is also possible to vary the arrangement of the elementary granules, hence the compactness of the beads, in order to obtain polymers of various apparent density.

This possibility of action on the bead structure permits to obtain resins adapted as well as possible to the end applications, without modifying other characteristics of the polymer as in the case of suspension polymerization when the nature of the protective colloid is changed.

- high density, coarse granulometry: rigid extrusion

- high density, fine granulometry: rigid calendering
- medium density, coarse granulometry: plastified extrusion
- medium density, medium granulometry: plastified calendering.

In all cases, bulk resins of PVC are characterized by a good porosity of the beads due to its structure and they are particularly suitable for the absorption of stabilizers, plastifiers and other ingredients.

2.2 Particle generation and evolution

The particle of bulk PVC is characterized by a structure radically different from that of the suspension PVC, due to the absence of the protective colloid. The bulk PVC particle with 80-200 microns diameter, is constituted by the direct and isotropic juxtaposition of granules having 0.5-1.0 microns diameter, which are homogeneous in dimensions and in structure.

Whatever the conditions of polymerization, the granules apparently keep constant dimensions. Their arrangement determines the morphological characteristics of the polymer. The association of the micronic granules, which is different according to the type of polymerization and of drying, determines the characteristics in the use of PVC resins.

In order to explain this microstructure it is necessary to examine what happens in the course of bulk polymerization of vinyl chloride and during the formation of the polymer particles. The

reaction is a free radical chain growth polymerization, the initiator generally being an organic peroxide soluble in the monomer. The vinyl chloride including the initiator in solution is rapidly brought to the temperature at which polymerization must take place. Even before the temperature level is reached, fine particles precipitate and create an opalescence.

They then progressively make the liquid more opaque. This opaqueness is due to the polymer chains insoluble in the monomer, which remain unassociated as long as their concentration remains low (less than 1% with respect to the monomer).

As the polymerization continues, the concentration of elementary particles increases and a phenomenon of polymer chain association can be recognized, which gives birth to the elementary granules.

The elementary granule is the smallest particle visible in the PVC structure under the electron microscope (Figures (2) and (3)).

In a recent work, Boissel and Fischer reported experiments at various temperatures between 20 and 60°C (3).

The first particles they observed in polymerizations at 50°C, are substantially spherical granules, with diameters below 0.25 to 0.35 μm (after removal of vinyl chloride). At lower temperatures, the presence of a substructure generates irregular geometries, and the particles are no longer spherical.

Given Boissel's experimental conditions, the granules form infinitely stable suspensions, as the flocculation described by Mickley (4) only occurs under different conditions. These granules continue their growth keeping a very uniform size distribution till a critical conversion is reached. At that time, the distribution ceases to be uniform, and a second nucleation occurs, with formation of particles much bigger in size.

The above mentioned critical conversion will depend strongly on the type and speed of agitation. This point is of major importance, as it makes possible an explanation of several differences with previously published work by Mickley (4), Cotman (5) and Bort (6).

Actually the experiments described in these publications are based on polymerization in a non agitated medium (sealed tube or dilatometer), with low volumes limiting the influence of thermal convection currents which may agitate the reaction medium.

In these conditions, it is certainly true that the critical conversion for agglomeration is likely to be very high, which explains why these authors mentioned above were able to observe uniform spherical granules at conversions above 0.1%.

The different stages of the start of the polymerization may be summarized as follows. The precipitated macromolecules initially formed, will constitute particles of about 0.01 μm diameter, that remain in stable suspension in the monomer. These granules will subsequently grow uniformly, without any formation of new particles,

up to a critical conversion, which depends on agitation and decreases when the intensity of agitation rises. In this stage, the size of these granules does not exceed 1 μm, according to Mickley (4) in the absence of agitation; and 0.2 to 0.3 μm in a highly agitated medium.

Then, a second nucleation occurs, and the granules agglomerate to form the final particles (Figures (2) and (3)).

As a conclusion, the mechanism by which the 1 μm particles or granules are generated, is not entirely clear. The extreme sensitivity to the agitation conditions and temperature, makes experimental reproducibility very difficult. General agreement does exist that those primary particles are created at conversions well below 1%.

Therefore, for the purposes of a model, the description of all interactions between oligomers in the very early stages of reaction can be disregarded, and instead to assume spontaneous generation of particles or granules with diameters in the order of 1 μm.

2.3 A history of different models

We will enumerate the most important contributions to the elucidation of the kinetic mechanism, which exhibits not only a large number of chemical reactions but the additional complication of its heterogeneous character. Starting with one liquid monomer phase, the system reaches the highest conversions with the coexistence of three phases: liquid and gaseous monomer and solid polymer.

Bengough and Norrish (7) formulated a model for heterogeneous bulk polymerization and then compared the experimental results with the theoretical calculations based on the model.

They observed a period of acceleration (over the first 40% conversion and different from the true gel effect at higher conversions) that was attributed to the cocatalytic effect of dead PVC and the initiator.

This cocatalytic effect was assumed due to chain transfer between growing polymer chains and molecules of dead polymer which produce free radicals in the surface of polymer and constitute stabilized centers of growth.

The reactivated polymer then continues to react with monomer, until the chain is terminated by transfer with monomer, thus producing mobile free radicals.

The rate of polymerization was assumed proportional to the 2/3 power of the weight of polymer because the catalytic effect would occur only at the external surface of the solid polymer. They also proposed that the rate of polymerization had an initiator dependence of 0.5 power of its concentration.

These authors took note of the presence of autoacceleration at lower conversions (cocatalytic effect), but the model has several weak points, as we will demonstrate later in our discussion of more recent contributions. We should point out that the arguments in favor of a cocatalytic effect concentrated only on the external

surface of particles are not satisfactory. More improved agglomeration mechanisms show that the particles originate by linkage of smaller units, and the external area becomes negligible compared to the total area developed by the highly porous material.

As a second weak aspect of the model, we should include the constant dependence of rate on initiator concentration. Transfer reactions are very important in vinyl chloride polymerization, and retardation effects imply an initiator dependence with powers ranging from 0.5 and 1.0, and possibly varying with conversion.

Breitenbach and Schindler (8) postulate in their model that precipitated polymer particles are swollen by the monomer, and growing radicals are inside them by both initiation in the particles as well as by entrance of chain radicals from the liquid monomeric phase. These radicals do not change the propagation rate but reduce the overall termination rate creating an autoacceleration effect.

This reduction in termination is represented by the equation:

$$\frac{1}{K_T} = \frac{1}{K_{TO}} + aC$$

where c is the conversion and a is a constant.

Under the assumption that both propagation and chain transfer rate constants have the same values in the liquid phase as in the solid particles, these authors arrived at an equation in which the degree of conversion is proportional to monomer concentration [M]

and to the 1/2 power of the initiator concentration [I]. At later stages of conversion the dependence is changed to be proportional to the second power of [M] and first power of [I], respectively.

Thus, conversion consists of two terms; one, characteristic of homogeneous polymerization and having 0.5 order dependence on initiator, and the second, related to the heterogeneous polymerization and depends on the initiator concentration to the power of 1.0.

These authors conclude that the overall reaction order in the initiator should be between 0.5 and 1.0, depending on the relative importance of the two terms. The hypotheses are supported by some experimental data showing dependence on initiator concentration to the power of 0.5 at short reaction times.

Magat (9) has made an attempt to apply the usual kinetic scheme (initiation, propagation, and mutual termination) to heterogeneous bulk polymerization by assuming that the quasi-steady state hypothesis cannot be applied in this case because of the strong decrease in termination rate. He also assumes that there are no chain transfer reactions to the monomer or polymer. Also, the termination constants are assumed to be low and equal in the liquid phase and in the polymer particles.

Mickley et al. (4) studied the polymerization of PVC in the presence of a solvent as well as in the bulk. For bulk polymerization, these authors give an expression for the rate, similar to that of Breitenbach and Schindler (8):

$$R_p = \kappa [M][I]^{\frac{1}{2}} + f(P)[I]^{\frac{1}{2}}$$

They argue that the first term is the contribution of homogeneous polymerization taking place simultaneously with heterogeneous polymerization represented by the second term. They observe that f(P) is proportional to P at low conversions and to $P^{2/3}$ at high conversions (this latter observation is in agreement with the work of Bengough and Norrish (7)).

According to these authors, the homogeneous component arises from the reaction of polymer radicals before they reach a critical size for coiling into primary polymer particles. Such particles will be very small and flocculate with others rapidly at a rate governed essentially by their rate of collision. By application of Von Smoluchowski's treatment of particle flocculation, it was postulated that virtually every particle was incorporated into a larger particle as soon as it is formed. Also, these small particles will sediment extremely slowly, and the frequency of collision between particles of very different sizes is much higher than that between aggregates of similar sizes.

Large particle clusters thus tend to scavenge the primary particles as they are produced. The system may be regarded as a precipitation process in which the primary particles, as they are formed, deposit on the larger particles present, which remain constant in number but increase in size. These authors assume that radical activity is trapped within a primary particle when it is incorporated

into a larger particle; or, if radical activity is transferred into particles from the liquid phase, a polymer concentration-dependent contribution to the polymerization rate can be expected. When the particles are small enough, the primary particles are supposed to have easy access to monomer or radicals actively present in solution, and a first order rate dependence on polymer concentration is postulated. However, when the agglomerates reach dimensions such that only the regions in the outer shell have effective access to the solution, a 2/3 power depen-ence (because of proportionality to surface area) will be found.

Thus, the main features of the mechanism proposed by these authors (4) include:

a) normal liquid phase kinetics

b) radical occlusion by coalescence

c) shallow penetration of radical activity into particles

d) negligible mutual termination in particles

e) escape of trapped radical activity by monomer transfer

f) limitation of short chain radical escape by propagation and transfer to polymer.

Cotman et al. (5) studied bulk polymerization techniques as well as particle properties to ascertain what control the latter exercise on rates of polymerization.

In their view, free radicals precipitate on or within agglomerates of partially swollen dead polymer. At the onset of polymerization, particles insoluble in the monomer are produced. At very

low conversions (less than 1%), particles grow into agglomerate units which increase further their sizes by deposition of polymer particles.

The rate of agglomeration of particles, quite high at low conversions, proceeds throughout the latter stages of polymerization, at a less rapid rate. Polymerization on solid polymer is characterized by autoacceleration rates due to a progressive reduction in termination rate.

This reduction is due to the fact that as the reaction continues and more polymer accumulates, there is a decrease in the mobility of free radicals produced by chain transfer and thus a lower probability of termination of growing chains.

At very low conversion, a decrease in polymerization rate occurs before autoacceleration sets in. This is explained by rapid particle coalescence which reduces the surface area and increases the termination rate by confining particles to a limited volume in close proximity.

The different kinetic steps which could take place in bulk polymerization, as proposed by these authors, are:

a) Initiation, propagation and termination of mobile soluble radicals.

b) Chain transfer to monomer by:

   i) mobile radicals

   ii) surface-entrapped free radicals on polymer.

c) Sticking of mobile free radicals on polymer (i.e., re-activation of dead polymer.

d) Propagation of radicals on polymer

e) Termination by:

i) Reaction of mobile free radical with "stuck" free radical.

ii) Mutual reaction of two "stuck" radicals.

Due to a lower mobility of the stuck free radicals, these termination steps are slower as compared to the termination of mobile soluble radicals. Also, these authors (5) indicate that the assumption of a "pseudo steady state" and use of a single valued rate constants is not valid.

In the mid-sixties Talamini et al. (10), (11), and as continuation of previous contributions (12), tried to give more specific consideration to the heterogeneous character of the polymerization. They clearly defined a scheme which allows for the occurrence of polymerization in both phases: the monomer rich phase, which contains practically no dissolved polymer, and the phase consisting of precipitated polymer, swollen with monomer. The initiator is assumed to distributed over both phases according to some partition law; therefore chain may be initiated in either phase.

However, the growing chains cannot change from one phase to the other during their lifetime, so that they will terminate in the same phase they were initiated. This scheme, which has been further specified and developed by Hamielec et al. (13), indicates

in its simplest form, a linear dependence of instantaneous rate on conversion:

$$\frac{dc}{dt} = a + bt \qquad (1)$$

The qualitative interpretation of the experimentally observed increase in rate with time (or conversion) is based in that polymerization proceeds faster in the polymer rich phase. Consequently, an increase in conversion will increase the amount of that phase, which will result, (according to the last equation), in higher rates of monomer consumption. We should emphasize that Talamini's model, despite its shortcomings, offered the best platform for all subsequent attempts to develop an improved model for bulk polymerization of vinyl chloride. This was probably the first work which accounted for the heterogeneity of the system by assuming two separate reacting phases. On the other hand, the most vulnerable aspect in Talamini's model is given by the complete absence of tranference of activity from one phase to the other.

Abdel-Alim and Hamielec (13) proposed a model which accurately predicts conversion and molecular weight distribution over a wide range.

Their model is essentially an extension of Talamini's model, with a number of modifications. Among them, there is a correction due to the volume change with conversion and the assumption that initiator is being consumed by a first order rate law. Also, the

concentration of polymer in the monomer rich phase is assumed to be negligible. Initiator concentrations in the two phases are assumed equal. They have proposed different polymerization rates depending on the conversion. When conversion is greater than a critical value indicating the disappearance of the monomer rich phase, they have introduced a change in the kinetic constants because at that stage, the termination and propagation rates will decrease due to a "gel effect."

These workers (13) have also given formulas for calculating the molecular weight distribution. They postulate that transfer to monomer plays an important part in controlling the molecular weight averages and that disproportionation is the dominant mode of termination.

Ugelstad et al. (14), (15), (16) retained the two phase character of the polymerization system and in addition allowed for the radical absorption and desorption to and from the polymer phase (particles) respectively.

These authors established a balance of radicals (activity carriers) in both phases allowing for absorption and desorption, and assuming a quasi steady state. The resulting model requires to adjust a parameter Q, defined as:

$$Q = \frac{K_a}{K_D} = \frac{[\dot{R}]_{POL}}{[\dot{R}]_{LIQ}}$$

where K_a and K_D are the absorption and desorption rate constants, respectively.

Q is obtained from experimental conversion versus time data, and measures the relation between radical absorption and desorption.

At high conversions, the equation takes the following asymptotic form:

$$\frac{dc}{dt} = C_1 + C_2\sqrt{c}$$

which exhibits a dependence of rate on the square root of conversion.

Olaj et al. (17), (18), (19) continued on the same kind of approach, but with much more refined description of the absorption and desorption processes.

It was assumed that radicals could be generated by initiator decay in both phases, monomer (liquid) and polymer (solid).

Radicals formed in the monomer rich phase will add monomer, thus being transformed into growing polymer chains. Due to the unfavorable thermodynamic conditions of the medium, they become insoluble and are finally incorporated into already existing particles. There, they may undergo further growth or deactivation by transfer or termination.

Radicals originated in the particles, will remain there, undergoing all possible reactions till termination.

Thus, it was assumed quantitative transfer of radical activity generated in the monomer phase to the solid polymer phase. Radicals

originated in the liquid phase, will only undergo propagation reactions.

The rate expression at low conversions, takes the following asymptotic form:

$$\frac{dc}{dt} = C_3 + C_4 \sqrt{c}$$

Ugelstad (14) tried to fit experimental data with his model, and concluded that good agreement was only possible for very high values of Q, i.e., $Q \geq 200$. Recalling the meaning of Q as ratio of absorption to desorption rates, it turns out that desorption rates from polymer particles are negligible. Under these limiting conditions, Ugelstad's model gives an expression for total rate of monomer consumption equivalent to Olaj's model (equation (3)). One should remember that the groups C_1, C_2, C_3 and C_4 are indeed functions of conversion as they include the volume growth of the phases. Therefore, the previous analogy between the two models is only evident when asymptotic conditions are imposed.

Ugelstad (15) has reported as an additional support to the previous discussion, that at 5% conversion, 98% of all radicals generated are present into the particles.

2.4 Review on experimental results

Most of the authors whose models we have discussed, have also performed experiments for interpreting their respective kinetic

models. Nevertheless, there has not been a single model which could actually fit all the experimental data for the complete range of conversions. Generally speaking, a particular model is valid for a certain range of conversions.

Only the most recent mechanical models proposed by Talamini (11), Hamielec (13) and Ugelstad (15) have been found to fit experimental data over a wide range of conversions (up to about 70%). However, these models involve empirical curve fitting and thus should be expected to fit the data reasonably well.

Bengough and Norrish (7) studied the autoacceleration in the rate of polymerization over the first 30-40% of reaction, over a whole range of temperatures from 33 to 75°C, and for varying initiator concentration. They found an acceleration in rate due to addition of dead PVC beads, and from their results they conclude that the catalytic effect of polymer is proportional to hte power of 2/3 as their model predicts. They also found that the degree of polymerization is independent of conversion and decreases with increasing temperature.

Arlman and Wagner (20) found that the autocatalytic effect also depends on the type of initiator. With benzoyl peroxide, the autocatalytic behavior was seen up to 20% conversion; but with 2,2 azoisobutyronitrile, it was observed up to 80% conversion. This observation is obviously explained by the different temperatures at which the experiments were run. The particular physical or

chemical properties of both types of initiator seem to have no influence on the autoacceleration.

Bengough and Norrish had observed that the catalytic effect of polymer is proportional to hte 2/3 power of its concentration, Mickley et al., have found that the autocatalytic effect depends on polymer concentration to the first power in the early stages of conversion and to 2/3 power at higher conversions. Cotman's experimental data fitted the Bengough-Norrish equation from 0.5% to 10% conversions and failed at higher conversions. A similar failure of Bengough and Norrish's model has also been reported by Arlman and Wagner (20), and Mickley et al. (4).

The Breitenbach and Schindler model (8) only agreed to a limited extent with the experimental observations of Cotman, while Magat's model correlates the data at higher conversions, but it does not fit the low conversion data.

From the experimental results quoted above, it is clear that none of the available models is entirely successful in representing the data over the entire range of experimental conditions, and none of them can predict the influence of the reactor operating conditions on the particle size distribution and particle structure, and indeed the influence of the particle morphology on the rate of conversion and molecular weight distribution of the polymer.

2.5 Chain transfer reactions

The bulk polymerization of vinyl chloride is a process in which transfer to monomer is dominant (21), (22), and exhibits,

from the very onset of the reaction, a continuous acceleration.

From previous reviews, it is easy to get a notion of the uncertainty when different authors attempt to find the cause for the observed acceleration by means of interactions between solid polymer and radicals.

In general, the result of this interaction is the creation of stabilized centers of growth, a concept that has been used to explain acceleration by an increase in propagation rate, or by a decrease in termination rate.

A typical and efficient method of characterizing this kind of reacting heterogeneous systems, consists in the addition of very reactive chain transfer agents like carbon tetrabromide or dodecyl mercaptan.

The normally observed effect is an increase of the initial rate, and a decrease or total elimination of the acceleration. Strong evidence has been given in references (21), (22) and (23).

Cotman has explained the elimination of autocatalysis in the early conversions, by assuming that the reaction of chain transfer agents with anchored (stabilized) radicals would produce smaller soluble units with increased mobility for diffusion and mutual termination.

Chemical reactivity aspects, like degradative chain transfer, have not been considered. Cotman also intended to explain the

increased intial rate by assuming that chains with lower molecular weight produced by the transfer, will provide greater surface area for capture of radicals and consequently, an increased initial rate.

Schindler and Breitenbach (8) argued that the autoacceleration was produced by the trapping of growing radicals within the precipitated polymer particles. This occlusion phenomenon would not change the propagation rate, but rather will decrease the termination rate as the reaction proceeds and more polymer is formed.

In a second work, Schindler and Breitenbach (21) presented more experimental evidence for the increase of initial rate and elimination of the acceleration in the presence of carbon tetrabromide, both in bulk and solution polymerization. In both cases, the polymerization proceeded at initial rates significantly higher than in the absence of chain transfer agent. With increasing concentrations of carbon tetrabromide, the rates soon reached what could be regarded as a limiting value, which was found independent of the kind of transfer agent and depended on the initiator concentration only. These findings were interpreted by the authors, to be due to the existence of degradative chain transfer to the monomer and an increase of the kinetic chain length by the added chain transfer agent.

The essence of the explanation postulated by these authors is given by the ability of the chain transfer agent to convert the less active monomer radicals ($MR^{\bullet}$) resulting from chain transfer,

into fully polymerization active radicals, which are able to propagate the kinetic scheme. ($TR^{\bullet}$ equivalent to $R^{\bullet}$):

degradative chain transfer	$\begin{cases} R + M \rightarrow MR + P \\ R + MR \rightarrow P \\ MR + MR \rightarrow P_2 \end{cases}$
chain transfer	$R + T \rightarrow TR + P$
chain promotion	$MR + T \rightarrow TR + \text{inactive}$

Recalling that the increase in initial rate is present in both homogeneous and heterogeneous polymerization, the explanations given by Cotman et al. (5) based on the role of the solid polymer phase, become irrelevant.

Considering an interpretation for the remaining acceleration phenomenon, Breitenbach's concept of different chemical reactivity (as discussed before) is still valid, because radicals originated as a consequence of the transfer, are expected to have smaller sizes and greater mobility for diffusion.

2.6 Solubility of vinyl chloride in poly-vinyl chloride

Different work previously discussed when dealing with particle generation models, and further studies by electron microscopy in references (24), (25), (26), have shown that porous particles of suspension or bulk PVC are agglomerates of primary or sub-particles in the order of 1 to 5 μm diameter.

Berens (26) has also found that an average size of the primary particles can be obtained from specific surface areas measured by

nitrogen adsorption. For a sphere of density ρ, the surface to weight ratio is $6/\rho d$. For PVC spheres, $\rho = 1.4$ g/cm^3, and results that:

$$\overline{ds} = \frac{4.29}{Sg}$$

where Sg is the specific surface area in m^2/g, and $\overline{d}_s$ is the surface average particle diameter in microns. Values determined in this way have shown good agreement with those obtained by electron microscopy.

Berens (27) also arrived at interesting conclusions by studying diffusion of monomer in suspension PVC. The results of sorption experiments corroborate his proposed model for diffusion in a uniform sphere having the diameter of the primary particles.

Thus, the uniform sphere model seems applicable to porous suspension PVC (and consequently to bulk); and the dimension controlling sorption rates, appears to be the size of the primary particles, not the external diameter of the agglomerate.

This means that diffusion of vinyl chloride monomer through the pores, and through any pericellular membrane around the gross particle, must be very rapid.

These important results were obtained for suspension PVC, but can be readily extended to the case of bulk PVC, which is known to present higher porosity.

On this basis, it seems possible to assume no diffusional control in the proposed model, at least while the monomer phase is present, valid for conversions lower than 67% at 50°C.

Solubility of vinyl chloride in PVC particles has been studied by Berens, under different ranges of temperature and pressure. Some of those results are presented in Figure (4). At higher temperatures and pressures, the data follow the Flory-Huggins equation very closely,

$$\ln \frac{P}{P_o} = \ln(1 - v_2) + v_2 + \chi v_2^2$$

where v_2 is the volume fraction of polymer in the vinyl chloride swollen PVC phase, and χ is the solvent-polymer interaction parameter.

The solid curve that fits all data between 30 and 60°C and at pressures close to 1 atm., was calculated with $\chi = 0.98$. In order to convert v_2 (volume fraction) to the units used by Berens, the following relation has to be used:

$$S = \left[\frac{\text{mg VCM}}{\text{g PVC}}\right] \frac{100(1 - v_2)\, d_m}{v_2 \quad d_p}$$

with densities of monomer and polymer, d_m and d_p, taken as 0.85 and 1.4 g/cm^2 respectively.

At pressures lower than 60% of saturation, the results do not follow the Flory-Huggins equation. Higher solubility values and a strong dependence upon time and PVC history is observed. These results are interpreted through the dual mode sorption concept of Michaelis, Vieth and Barrie (28). These authors consider the

solubility of a vapor in a glassy polymer to be the sum of a normal dissolution process, which contributes to a steadily increasing solubility as the vapor pressure increases, and a "hole filling process," which approaches a limiting saturation value with increasing pressure.

It is considered that the Flory-Huggins behavior observed at higher temperatures and pressures, represents the normal dissolution contribution over the entire range of vinyl chloride temperatures and pressures.

The additional solubility above the Flory-Huggins curve is attributed to the "hole filling process," saturation of the pores with increasing vinyl chloride pressure.

2.7 Some features of vinyl chloride polymerization at higher conversions: Gel effect and change in the monomer-polymer equilibrium conditions

We have already indicated that before changes in pressure occur, ordinary bulk and suspension vinyl chloride polymerization are characterized by a two phase system consisting of a nearly pure liquid monomer phase, and a monomer swollen polymer phase. The major part of the polymerization reactions occur in the polymer phase.

But as conversion increases, the capillary porous coagulation structure consisting of PVC primary particles has the effect of lowering the vinyl chloride vapor pressure with the result that the polymer

phase composition is altered while liquid monomer phase is still present.

According to studies of Kuchanov and Bort (6), while the liquid phase is present, the monomer will be distributed in the pores, and the filling of them will depend on the degree of conversion and on pore size distribution. At the moment a coagulation structure is formed, the pores are completely filled with monomer. As the degree of conversion increases, and as more monomer is utilized, some of the pores will be filled with gaseous monomer and others with liquid monomer.

Because of the positive angle of wetting of the polymer phase surface by a liquid monomer, the latter will tend, under the action of capillary forces, to fill the pores that have the smallest possible radii.

It appears that for any amount of liquid monomer phase, there will be a maximum pore radius r_{max} for pores filled with liquid monomer. Gaseous monomer will fill up all the other pores with larger radii.

Under thermodynamic equilibrium conditions, vinyl chloride will be distributed between gas, liquid and polymer phases in such a way that the chemical potential will be the same in all the three phases.

As conversion increases, the liquid phase is being consumed and r_{max} will be reduced. The relation between r_{max} and the

pressure, is given by Thompson's formula, which can be deduced from an energy balance in the capillary:

$$RT \ln \frac{P}{P_0} = \frac{2\sigma V}{r_{max}}$$

where P and P_0 are respectively the pressure of vinyl chloride vapor in a capillary of radius r_{max} and over a plane surface; σ is the surface tension, V is the specific volume of monomer, R is the gas constant and T the absolute temperature.

As the amount of polymer formed increases, r_{max} and P will decrease. The immediate effect will be an increase in viscosity and a reduction of the termination rate constant. The influence on the other kinetic steps like initiation or propagation will not be so significant, because their rate constants are less sensitive to diffusion factors that depend on the viscosity of the medium.

We have noted before when discussing vinyl chloride-PVC equilibrium, the strong sensitivity of solubility with pressure changes.

When Pm/Pmo = 0.96, solubility is only 85% of the saturation value.

At Pm/Pmo = 0.40, solubility decays to 15% of that observed at saturation conditions.

In current practice, vinyl chloride polymerization is not stopped when the liquid phase disappears, but at a substantial sub-saturation pressure, i.e., 70% of saturation pressure. Beside the

normal decrease in pressure that is verified at higher conversions, subsaturation conditions are sometimes programmed and imposed ex-professo. This is known in the literature as U polymerization, and several important changes in morphology, molecular weight and processing conditions are verified.

Sorvik (29) and Sorvik and Hjtertberg (30) have made important contributions on this topic. When polymerization is continued during subsaturation conditions, the molecular weight distribution is broadened due to an increase in both low and high molecular weight polymer. An extensive degree of long chain branching is also obtained.

At the actual pressure of 40% of saturation, solubility of vinyl chloride in poly-vinyl chloride is only 15% of the solubility at saturation pressure, which causes a substantial deswelling of the gel. The reduced monomer concentration will cause a decrease in the propagation rate, resulting in a lower overall rate.

Though the rate of initiator decomposition will not decrease with deswelling of the gel, the concentration of mobile oligomeric radicals will increase.

The increased radical concentration and the decreased mobility in the deswollen gel, should increase the tendency to mutual termination of oligo-radicals, thus increasing the content of low molecular weight polymer. On the other hand the increased immobilization will, per se, contribute to a reduced termination of macro-radicals and increase the possibility of formation of high molecular weight

material. The dense structure of the gel will also enhance reactions between radicals and polymer molecules, leading to long chain branching.

In conclusion, the U polymerization presents a simple means to prepare PVC with a substantial and controlled degree of "abnormal" structures, such as long chain branching, broad molecular weight, reduced porosity, etc.

2.8 Branching

Another controversial feature in the mechanism of heterogeneous polymerization is with regard to chain branching. The Bengough and Norrish mechanism (7) assumes chain transfer to polymer and therefore postulates that long branches must be formed in the polymer. Cotman (5) found that the extent of branching in commercial PVC is about one branch per 50 monomer units. George et al. (31) found that branching was dependent on the temperature and showed specifically that at -40°C there was almost no branching. Boccato et al. (32) also studied the branching of PVC. They found that samples prepared at 50°C have approximately one side chain for every 60 carbon atoms, whereas samples prepared at temperatures below -60°C are practically linear.

Other authors have reported similar results. However, they could not determine clearly, if branching is of a short or long type.

Long chain branching may be originated by transfer between growing radicals and dead polymer, or by addition of terminal

double bonds (of preformed molecules) to a growing radical. On the other side, short chain branching implies intramolecular transfer through intermediate formation of a five or six membered ring; or head to head addition followed by radical isomerization to produce $\_\_CH_2Cl$ groups (33). Therefore, the conclusion we can draw from this is that, although branching is confirmed, only the short type seems to predominate under normal reaction conditions. Consequently, chain transfer to polymer mechanisms proposed by Bengough and Norrish, Mickley and Cotman are possibly incorrect.

Some more recent work by Abbas et al. (34), Park (35) and Abbas (36) allowed a better understanding with quantitative data. By the use of C^{13} NMR, it was demonstrated that the short branches in PVC are pendent chloromethyl groups. The extent of short branching is about 3 methyl groups per 1000 carbons. The number of branches does not change significantly with polymerization temperature (40 - 75°C). There is also some evidence for long branches (more than 6 carbon atoms long). The content of long chain branching does not exceed 1 branch per 1000 carbons. The proportion of long chain branching is known to increase under subsaturation conditions or monomer starving at high conversions (29), (30), but under normal reactor operation, branching can be obviated without affecting the performance of the kinetic model.

2.9 Reaction order with respect to initiator

The reaction order with respect to initiator has been proposed as a value between 0.5 and 1.0 by many authors. Bengough and Norrish (7) found a value of 0.5 in polymerization carried out at 40°C with benzoyl peroxide as initiator. Breitenbach and Schindler (8) found an order of 0.58 at 30 to 60°C using the same initiator. Danusso (37) observed different reaction orders for initiator with changing conversion; i.e., he found reaction orders of 0.46 to 0.52 from 2-8% conversion, while at 30% conversion the reaction orders had values between 0.50 and 0.54. Mickley et al., found that the order was approximately 0.5. Hamielec assumed a dependence of 0.5 on initiator concentration and was able to fit his data.

Breitenbach and Schindler (21) have demonstrated the presence of degradative chain transfer to monomer in vinyl chloride polymerization, and this implies that in an homogeneous system, the order with respect to initiator has boundaries given by 0.5 and 1.0 (21), (38).

But in the case of heterogeneous polymerizations in which the phases themselves evolve in time, the dependence becomes much more complicated and possibly changing with conversion. This will obviously depend on the set of chemical reactions imposed, the particular description of the heterogeneous system and interaction between phases. Further emphasis on this aspect will be given on subsequent discussions.

C H A P T E R I I I

THE MATHEMATICAL APPROACH

3.1 The proposed kinetic model

In an attempt to describe this polymerization process by a more efficient model, two aspects were emphasized:

1) Predominium of reaction in particles. As reported by Ugelstad (15) at 5% conversion, 98% of the propagation reactions occur into the particles. This point was already treated in detail when comparing the coincidence in results between Ugelstad and Olaj's models, and their comparisons with experimental data.

2) Transfer mechanism and the response to chain transfer agents. It was followed in this sense, similar criteria to those de-developed by Breitenbach and Schindler (21), where the transfer capacity of different radicals is explained not only in physical terms (like radical size or formation of stabilized centers of growth), but also by postulating different chemical reactivities of the spices involved in the transfer.

Similarly to Olaj's description, radicals can be generated in both phases, but those from the monomer (liquid phase) will only undergo propagation till reaching critical length for insolubility and precipitation. Finally, these radicals are incorporated to already existing particles, where they are inactivated either by transfer or mutual termination.

In other terms, it is assumed that there is quantitative transfer of activity from the monomer to the solid polymer phase.

Chains originated into the particles will remain there and undergo all the reactions we have postulated, till termination. The possibility of desorption could only take place in the very onset of the polymerization, as described by Olaj (18).

From the results of Cotman (5) and lately of Boissel (3) it is known that between 0.5 and 1.0% conversion there is a sudden decrease in the total number of particles owed to an agglomeration phenomenon. It implies a serious increase in the ratio radical-particle, which from now and on will remain essentially constant.

The possibility of a desorption process could only be given before the nucleation step, in conversions lower than 1%. Its consideration is unjustified for the purpose of this model.

The residence time of the oligomers undergoing propagation in the liquid phase is too short when compared to the rest of the processes, implying that transfer of that radical activity will be only by agglomeration (no diffusional mechanisms).

The complete set of chemical reactions, is stated as follows:

initiation	$I \longrightarrow 2IR$ $IR + M \longrightarrow R$	overall rate:	$2f K_1 [I]$
propagation	$R + M \longrightarrow R$		$K_2 [R][M]$
termination	$R + R \longrightarrow P$		$K_3 [R]^2$
degradative chain transfer	$R + M \longrightarrow MR + P$		$K_4 [R][M]$
	$R + MR \longrightarrow P$		$K_5 [R][MR]$
	$MR + MR \longrightarrow$	(inactive)	$K_6 [MR]^2$

reinitiation	$MR + M \longrightarrow R$	$K_{1a}[MR][M]$
transfer to transfer agent	$R + T \longrightarrow TR + P$	$K_7[R][T]$
chain promotion	$MR + T \longrightarrow$ (inactive)	$K_8[MR][T]$

Recalling that initiation and propagation are the only kinetic steps conceived in the liquid phase, it is possible to write the following balances:

Radicals balance in liquid phase (in moles)

$$\frac{d\dot{R}_L}{dt} = \rho_{iL} - K_a \dot{R}_L \tag{4}$$

Radicals balance in particles (in moles) (5)

$$\frac{dR_P}{dt} = \rho_{iP} + K_a \dot{R}_L - K_3[R]_p^2 V_p - K_4[R][M]V_P - K_8[MR][T]V_P + K_{La}[MR][M]V_P - K_5[MR][R]_p V_p$$

Balance of MR• radicals

$$\frac{dMR}{dt} = K_4[R][M]V_P - K_5[MR][R]V_P - K_6[MR]^2 V_P - K_8[MR][T]V_P - K_{1a}[MR][M]V_P = 0 \tag{6}$$

By addition of the three previous equations, and assuming for k_5 (21) the geometric mean value between k_3 and k_6 (cross-termination), it is possible to get an expression for radicals MR• as a function of R•:

$$[MR] = \left(\frac{\rho_{iL} + \rho_{iP}}{V_P K_6}\right)^{\frac{1}{2}} - \left(\frac{K_3}{K_6}\right)^{\frac{1}{2}}[R] \tag{8}$$

Steady state assumptions in equations (4) and (5) permit the following combination of the two:

$$\frac{\rho_{iL} + \rho_{iP}}{V_p} - K_3[R]^2 - K_4[R][M] - (K_3 K_6)^{\frac{1}{2}}[R][MR] +$$

$$+ K_{1a}[MR][M] + K_8[MR][T] = 0$$

Replacing the value of MR• from equation (8), a final value for radical concentration R• is obtained:

$$[R]_p = \frac{\frac{\rho_{iL}+\rho_{iP}}{V_P} + K_8[T]\left(\frac{\rho_{iL}+\rho_{iP}}{V_P K_6}\right)^{\frac{1}{2}} + K_{1a}[M]\left(\frac{\rho_{iL}+\rho_{iP}}{V_P K_6}\right)^{\frac{1}{2}}}{K_4[M] + K_3^{\frac{1}{2}}\left(\frac{\rho_{iL}+\rho_{iP}}{V_P}\right)^{\frac{1}{2}} + K_{1a}[M]\left(\frac{K_3}{K_6}\right)^{\frac{1}{2}} + K_8[T]\left(\frac{K_3}{K_6}\right)^{\frac{1}{2}}}$$

Rate of monomer consumption (in moles)

$$\frac{dM}{dt} = K_2[R]_L[M]_L V_L + K_2[R]_p[M]_p V_p + K_4[R]_p[M]_p V_p +$$

$$+ K_{1a}[M]V_p\left(\frac{\rho_{iL} + \rho_{iP}}{V_p K_6}\right)^{\frac{1}{2}} - K_{1a}\left(\frac{K_3}{K_6}\right)^{\frac{1}{2}}[R][M]V_p \qquad (10)$$

Replacing $[R^\cdot]_p$ by its expression (equation (9)), one obtains:

$$\frac{dM}{dt} = K_2[R]_L[M]_L V_L + \left[K_2 + K_4 - K_{1a}\left(\frac{K_3}{K_6}\right)^{\frac{1}{2}}\right]$$

$$\left\{\frac{\left(\frac{\rho_{iL}+\rho_{iP}}{V_P}\right) + K_{1a}[M]\left(\frac{\rho_{iL}+\rho_{iP}}{V_P K_6}\right)^{\frac{1}{2}} + K_8[T]\left(\frac{\rho_{iL}+\rho_{iP}}{V_P K_6}\right)^{\frac{1}{2}}}{(K_3)^{\frac{1}{2}}\left(\frac{\rho_{iL}+\rho_{iP}}{V_P}\right)^{\frac{1}{2}} + K_4[M] + K_{1a}[M]\left(\frac{K_3}{K_6}\right)^{\frac{1}{2}} + K_8[T]\left(\frac{K_3}{K_6}\right)^{\frac{1}{2}}}\right\}[M]_p V_p +$$

$$+ K_{1a}\left(\rho_{iL} + \rho_{iP}\right)^{\frac{1}{2}}[M]_p V_p \qquad (11)$$

If a parameter A is used to establish the monomer-polymer equilibrium, as

$$A = \frac{\text{monomer weight in polymer phase}}{\text{polymer weight in polymer phase}}$$

it is possible to write expressions for the volumes of both phases as a function of conversion:

(total moles in liquid phase) $V_L[M]_L = M_0 - M_0 C - M_0 A C$

(total moles in polymer phase) $V_P[M]_P = M_0 A C$

Assuming volume additivity in the particles,

$$V_P = \frac{m_M}{d_m} + \frac{m_P}{d_P} = \frac{A M_0 C}{d_m} + \frac{A M_0 C}{d_P}$$

(volume of liquid phase) $V_L = V_0 (1 - C - AC)$

(volume of polymer phase) $V_P = V_0 \left(A + \frac{d_m}{d_P} \right) C$

(total volume) $V_{TOT} = V_L + V_P = V_0 \left(1 + \frac{d_m}{d_P} C - C \right)$

The steady state balance (equation (4)), provides an expression for the concentration of radicals $[R^\cdot]_L$:

$$\rho_{iL} = 2K_1 [I]_L V_L = K_a [R]_L V_L \quad ; \quad [R]_L = \frac{2K_1 [I]_L}{K_a}$$

Recalling the previous assumption of uniform distribution of initiator in both reacting phases, one observes that

$$\rho_{iL} = \rho_{iP} = 2K_1 [I]_L V_L = 2K_1 [I]_P V_P$$

$$[I]_L = [I]_P = [I]_0 e^{-K_1 t}$$

To being the total initial moles of initiator. The fractional conversion versus time can be obtained by introducing all the above expressions in equation (11), and then dividing by the total initial number of moles M_0. With the simpler notation

$$[T] = CBR4 \qquad e^{-K_1 t} = QB \qquad \left(\frac{dm}{dp} + A\right) = QA$$

the fractional conversion results as

$$\frac{dC}{dt} = Q_1 + Q_2 \frac{(Q_3 + Q_4 + Q_5)}{(Q_6 + Q_7 + Q_8)} + Q_9 \tag{12}$$

where

$$Q_1 = \frac{2 K_1 K_2 IO \cdot QB}{Ka} \cdot \frac{(1 - C - AC)}{(1 + C(QA - A - 1))}$$

$$Q_2 = K_2 + K_4 - K_1 a \left(\frac{K_3}{K_6}\right)^{\frac{1}{2}}$$

$$Q_3 = \frac{2}{QA} \cdot K_1 \cdot IO \cdot A \cdot QB \cdot C^{\frac{1}{2}}$$

$$Q_4 = A^2 \cdot MO \cdot \frac{K_1 a}{QA} \cdot \left(\frac{2 K_1 \cdot IO \cdot QB}{QA \cdot K_6}\right)^{\frac{1}{2}} \cdot C$$

$$Q_5 = K_8 \cdot CBR4 \cdot A \cdot 2\left(\frac{K_1 \cdot IO \cdot QB}{QA \cdot K_6}\right)^{\frac{1}{2}} \cdot C$$

$$Q_6 = \left(K_{1a} + \left(\frac{K_3}{K_6}\right)^{\frac{1}{2}} + K_4 \right) . MO . \frac{A}{QA} . C^{\frac{1}{2}}$$

$$Q_7 = \left[2 . K_1 . K_3 . IO . (QB / QA) \right]^{\frac{1}{2}}$$

$$Q_8 = K_8 . CBR4 . \left(\frac{K_3 . C}{K_6} \right)^{\frac{1}{2}}$$

$$Q_9 = K_{1a} . A . \left(\frac{2 . K_1 . IO . QB . C}{QA . K_6} \right)^{\frac{1}{2}}$$

3.2 The agglomeration model

The process of agglomeration or coagulation in a spatially homogeneous system, in the approximation of pairwise collisions for a given initial distribution without taking account of spontaneous generation or breakdown of particles, is described by the kinetic equation:

$$\frac{\partial F}{\partial t}(V,t) = \frac{1}{2} \int_0^V K_c (E, V-v, v) F(V-v) F(v) dv - F(V,t) \int_0^\infty K_c (E, V, v) F(v) dv \qquad (13)$$

where F(V,t) is the density of the distribution of the particles over the volume V at time t.

K_c (V, V-v, E) is the kernel of the equation, characterizing the probability of coagulation of two particles having volumes V and V-v, in unit volume, in unit time.

With the study of the kinetics of coagulation, there arises the problem of determining the kernel of the governing equation K_c(V, V-v, E) that will contain all information about hydrodynamic and electric interactions under the given physical conditions.

Golovin (42), Scott (43), and Melzak (44) have studied different models for coagulation of droplets that are variations of equation (13) by assuming different types of dependence of the kernel on particle size, and on a diversity of initial conditions (distributions). A thorough review in colloid science and particulate systems, shows that at the present time there is only one theory, that of DLVO (Derjaguin, Landau, Verwey and Overbeek) (45) that may be useful in predicting the functionality of the kernel in the coagulation equation, or giving some criteria about the stability of the system.

We will briefly point out its most important aspects, and show how this rather simple model permits to account for hydrodynamic and electric interactions. The DLVO theory is concerned almost exclusively with dispersons of particles of uniform size.

The problem of interaction in a particulate system can be treated by considering either the energy of interaction or the force

derived from that energy. In the present case, the energy treatment is preferred, among other things, because the interaction has to be compared to the energy of the Brownian motion. The potential of interaction is considered to consist of two components (45), (46):

1) that arising from overlap of electrical double layers, and leading to repulsion, Vr,
2) that arising from London--van der Waals dispersion forces and leading to attraction, Va, such that

$$V = Va + Vr$$

The general character of the curve of total interaction V, can be easily deduced from the properties of the repulsion and the attraction.

The repulsion has the features of an exponential function with a range of the order of the thickness of the double layer. It remains finite for all values of the distance between the particles. The attraction however decreases as some inverse power of distance. For very small distances it goes to very large negative values (Figure 5).

Consequently, the attraction will predominate at very small and at very large distances. At intermediate distances the repulsion may be important, but whether this is really the case, will depend upon the actual numerical values of the attractive and repulsive forces.

It should be noted that even if both surface potentials are of like sign, attraction forces will be generated when both potentials are different in magnitude. As particles come close, there is a critical distance at which there will be a change from repulsion to attraction (Figure (5)). Further comparison for all possible cases, are given in references (45), (46), (52), and (54).

Various treatments have been put forward for the calculation of Va and Vr, which depend on the size and shape of the particle, the dielectric constant of the particle and the medium, and, in the case of Vr, also on the electrolyte concentration and the surface potential of the particle. General reviews are given in reference (45) and (46).

The course of coagulation with time is determined by two factors, the Brownian motion of the particles and their interaction when they are close together. The simplest case can be reproduced at very high dilution, so that the repulsion forces can be neglected. As a further simplification, the attraction effects can be represented by a sphere of action surrounding each particle. Any second particle entering this sphere of action, will cause the irreversible coagulation of the two particles. This implies to have replaced the London-Van der Waals attraction potential by an infinitely deep well, with a vertical wall.

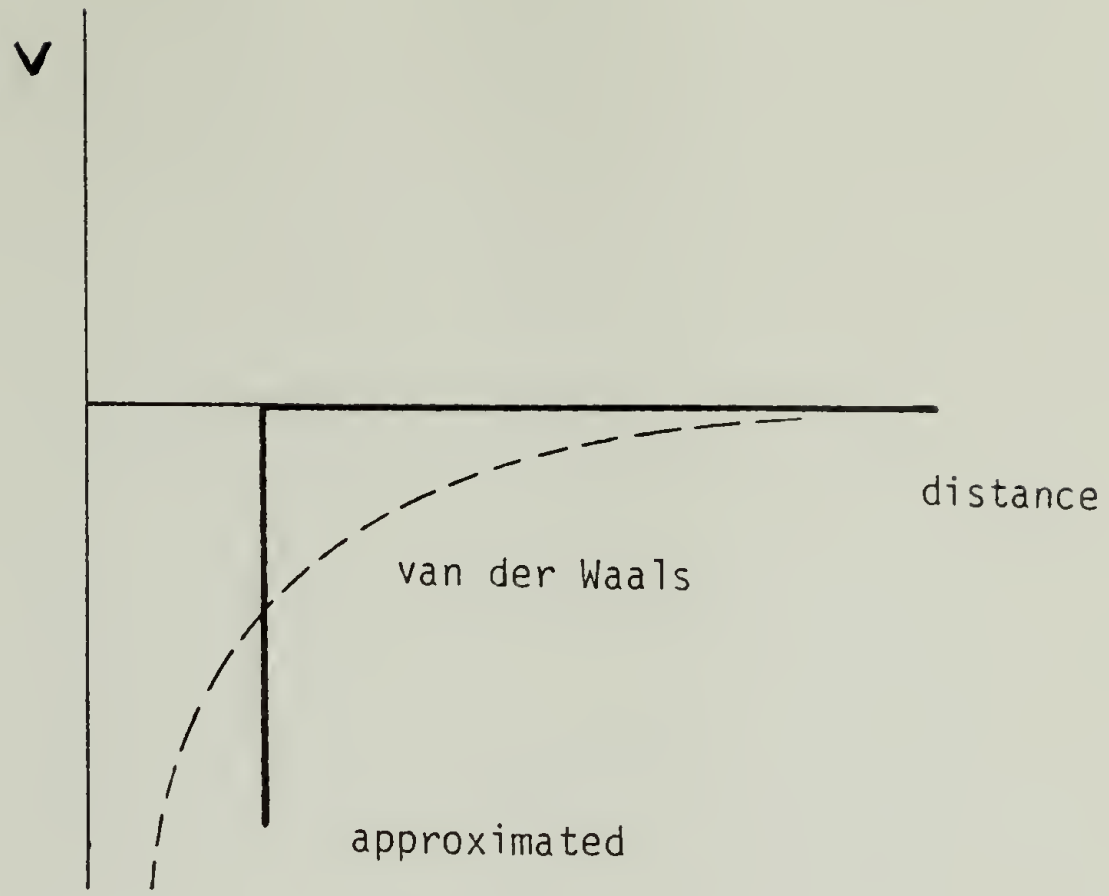

Every encounter of two particles leads to a permanent contact, determined only by Brownian movement, and that is defined as a fast coagulation.

Von Smoluchowsky (47), (48) has solved this problem by assuming one particle fixed in the origin of coordinates and calculating the number of collisions in the course of time.

The problem became reduced to a diffusion process under the Fick's second equation

$$\frac{\partial \nu}{\partial t} = D \nabla^2 \nu$$

and

$$\begin{cases} t = 0 : & \nu = \nu_0 & r > R \\ t > 0 : & \nu = 0 & r = R \end{cases}$$

ν_0 = total initial number of particles per unit value.

r = distance from the center of coordinates

R = distance between the centers of two particles

a = radius of a particle

For $t \gg R^2/D$ a steady state can be assumed and in this case, the number J of particles diffusing through any closed surface in the direction of a central one, must be constant. Consequently, the process can be more easily described by Fick's first equation, which for a sphere around the origin states:

$$J = D\, 4\pi r^2 \frac{\partial \nu}{\partial r}$$

The solution of this equation satisfying the conditions $\nu=\nu_0$ for $r=\infty$ is

$$\nu = \nu_0 - \frac{J}{D} \cdot \frac{1}{4\pi r}$$

With the aid of the condition $\nu=o$ for $r=R$, the number of collisions with the central particle is found to be

$$J = 4\pi D R \nu_0$$

If the central particle is also subject to Brownian motion, the diffusion constant is now

$$D_{12} = D_1 + D_2$$

or when the particles are of equal size,

$$D_{11} = 2 D_1$$

(The diffusion constant is related to the mean square of the displacement in one direction by the equation

$$D = \frac{\overline{x^2}}{2t}$$

The relative displacement of two particles is given by $x_1 - x_2$ and so the relative diffusion constant by

$$D_{12} = \frac{\overline{(x_1 - x_2)^2}}{2t} = \frac{\overline{x_1^2}}{2t} - \frac{2\overline{x_1 x_2}}{2t} + \frac{\overline{x_2^2}}{2t} = D_1 + D_2$$

as the average value of $x_1 x_2$ is zero).

The number of particles colliding with one individual particle is equal to $8\pi D r \nu_0$ and the rate of disappearance of primary particles is given by

$$\frac{d\nu}{dt} = 8\pi D R N_a \nu^2$$

which shows that coagulation proceeds as a bimolecular reaction, the rate constant of which can be expressed in terms of known quantities.

When the last equation is written in molar concentrations we get:

$$-\frac{dc}{dt} = 8\pi D R N_a c^2$$

with a bimolecular constant

$$k_c = 8\pi D R N_a$$

Substituting R=2a and $D = \frac{kT}{6\pi\eta a}$ (according to Stokes-Einstein), we find for k_c:

$$k_c = \frac{8 N_a k T}{3\eta}$$

which is about 6×10^{12} for room temperature and the viscosity of water, just the expected order of magnitude for a bimolecular collision factor.

Slow coagulation

Fuchs in 1934 (49) described a more general case that allowed for the existence of an electric potential barrier, and his results permitted to establish some criteria for determining the stability of a colloidal system.

The presence of energy barriers will reduce the number of effective collisions, situation defined as slow coagulation.

The rate of collision was formulated according to the following transport equation:

$$\frac{\partial c}{\partial t} = D \nabla^2 c + (-B) \nabla F c$$

where c is the population of particles per unit volume, F is the interacting force, and B is the mobility in that medium.

For a spherical symmetrical coordinate system, the following form of the equation is obtained:

$$\frac{\partial c}{\partial t} = \frac{1}{r^2} \frac{\partial}{\partial r} \left(D r^2 \frac{\partial c}{\partial r} \left(D r^2 \frac{\partial c}{\partial r} - B r^2 F(r) c \right) \right.$$

For a steady state approximation and with boundary conditions

$$r = \quad : \quad c = 0$$

$$r = \infty \; : \quad c = c_0$$

$$C = \exp\left(\frac{B}{D} \int_{\infty}^{r} F \, dr \right) \left[C_0 + \frac{J}{D} \int_{\infty}^{r} \frac{1}{r^2} \exp\left(-\frac{B}{D} \int_{\infty}^{r} F \, dr \right) dr \right]$$

where

$$J = \frac{D C_0}{\int_{2a}^{\infty} \left[\frac{1}{r^2} \exp\left(-\frac{B}{D} \int_{\infty}^{r} F(r) \, dr \right) \right] dr}$$

Using B=D/kT and dV/dr=-F, Overbeek obtained the following equation:

$$G = 8\pi J = \frac{8\pi D C_0}{\int_{2a}^{\infty} \frac{1}{r^2} \exp\left(\frac{V}{kT} \right) dr}$$

where G is the number of incoming particles toward the center particle for collision per second. He proceeded the extreme case further: i.e., when there is no interaction energy barrier, so that the collision depends upon diffusion only, then:

$$G_{MAX} = \frac{8\pi D C_0}{1/2a} = 2a\,8\pi D C_0$$

Now the collision fraction, 1/W, is defined as:

$$\frac{1}{W} = \frac{G}{G_{MAX}} = \frac{1}{2a\int_{2a}^{\infty} \frac{1}{r^2} \exp\left(\frac{V}{KT}\right) dr} \simeq 2K a \exp\left(-\frac{V_{MAX}}{KT}\right)$$

The collision fraction 1/W, (which was named as the stability ratio), has such a meaning as the fraction of collisions happening among the particles which have overcome the interaction (repulsive) energy barrier, and so, when there is not energy barrier, the collision fraction becomes 1/W=1, and the particles collide by diffusion only.

Thus, the rate of coalescence can be written as

$$\frac{dc}{dt} = \left\{ K_c C^2 \right\} \cdot \frac{1}{W}$$

where the coefficient of coalescence rate K_c, is based on diffusion only.

The last equation indicates that the rate of agglomeration is a product of the diffusional collision of particles times the collision fraction due to the interaction energy barrier.

Extension of the DLVO theory to polydisperse systems (heterocoagulation) is governed by the same principal factors controlling agglomeration of identical particles.

However, in the case of different sizes, the electrostatic interactions will occur in the domain of asymmetric electrical double layers, which involves a more detailed and complicated study.

Most of the contributions in this field with the development of mathematical expressions for the potentials (50), (51). An excellent more recent review on heterocoagulation is given by Usui (52).

It should be remarked that even if both surface potentials are of like sign, attraction forces will be generated when both potentials are different in magnitude.

An extension of equation (53) to heterogeneous systems, results as follows:

$$\frac{\partial c_i}{\partial t} = D_{ij} \nabla^2 c_i - B_{ij} (F_{ij} c_i)$$

and defining as before a diffusion coefficient D_{ij} for two particles of radii a_i and a_j as

$$D_{ij} = D_i + D_j = \frac{KT}{\eta 6\pi} \left(\frac{1}{a_i} + \frac{1}{a_j} \right)$$

and a mobility

$$B_{ij} = D_{ij} / KT$$

With an analogous approach to that previously used in defining the stability ratio, it is readily obtained, for two particles of radii a_i and a_j that

$$\frac{d C_{ij}}{dt} = \frac{4KT}{3\eta\pi K^3} \left(\frac{1}{a_i a_j} \right) \exp\left(\frac{V_{MAX}}{KT} \right) C_i C_j$$

or

$$\frac{dC_{ij}}{dt} = K_C (a_i, a_j, V)\, C_i C_j$$

The DLVO theory has been verified in many cases, specially in emulsions, where the interface area and shape of the particles is well know, and the surface charge can be modified with the addition of electrolites (54), (55) and (56). Charges and mobilities can be measured by a number of techniques like electrophoresis or diffusion through membranes.

In vinyl chloride bulk polymerization, the situation is much more complicated. Agglomeration is developed till completion while chemical reactions are occurring. It is well known that PVC granules, immersed in vinyl chloride, have no tendency to agglomeration,

and can remain indefinitely unperturbed. But during chemical reaction, interaction forces will be generated by the charge of all radical species present.

Once the agglomeration is produced, vinculation between particles becomes more complex because growing polymer chains will cause irreversible anchoring of the colliding units.

Therefore, measuring the evolution of particle properties in a system under reaction implies additional complexity. Though there is current work done in this field, no definitive experimental data have been found in the open literature.

The results obtained from the previous theoretical analysis for an expression for K_c (agglomeration) will be followed throughout the whole development of the model equations. It provides, as explained before, an inverse relation between coagulation rate and particle size, (equation 14)), what dictates that smaller particles will coagulate faster, as they will be trapped by already grown agglomerates. Beside the kinetic or diffusional aspect, K_c predicts a potential barrier in the term $e^{-v/kT}$. Though V is not accurately known, it can be estimated and bounded by comparison with surface potentials in some other systems, or through the number of radicals and number of particles in the reaction medium. The resulting values for K_c are well within the magnitude expected for a coagulation constant.

3.3 Population balance equations

The formulation of the model will basically require population balance methods to develop balances for the particle distribution and related quantities. The general population balance equation for a particulate siste system in which the individual particle property is a vector $X=(x_1, x_2, \ldots\ldots x_n)$ with some range V in the n-dimensional property space is given by (57):

$$\frac{\partial W_x}{\partial t} + \nabla \cdot [\dot{X} W] = h(W_x, t) \qquad (15)$$

In equation (15), W(x,t) is the density of the distribution of particles in V and t; $\dot{X}$ is the rate of change of property X; the operator on the left hand size of equation (15) is a "continuity" operator and the nonzero right hand side reflects the possibility of spontaneous creation and destruction of particles in this space.

The functional $h(W_X,t)$ represents the net rate of appearance of new particles with property X. The form of the functional $h(W_X,t)$ depends on the specific mechanism by which particles appear and disappear from the system.

In order to develop a detailed quantitative model, it is necessary to formulate the population balance equations for the following particle property distributions (58), (59), (60), (61):

$F(V)$: continuous univariate total particle size distribution function, with which $F(V)dV$ gives the total number of particles per unit volume, of size V to V+dV.

$f_i(V)$: bivariate radical number distribution function with a continuous variable of particle size V and a discrete variable of radical number i, with which $f_i(V)dV$ gives the number of particles (per unit volume) of size V to V+dV having i radicals into them.

$f_n(i,V)$: trivariate live chain length weight (i) distribution function with a continuous variable of particle size V and discrete variables of radical number i and live polymer chain length n, with which $f_n(i,V)dV$ gives the number of radicals of chain length n in the number of particles (per unit volume) of size V to V+dV having i growing radicals.

$G_n(i,V)$: trivariate dead chain length weight (number of dead polymers) distribution function with a continuous variable of particle size V and discrete variables of radical number i and dead polymer chain length n, with which $G_n(i,V)dV$ gives the number of dead polymers of chain length n in the number of particles (per unit volume) of size V to V+dV having i growing radicals.

Among the above distribution functions of particle population, both the total particle size distribution function $F(V)$ and the radical number distribution function $f_i(V)$ are defined in terms of the number density of the particle population. However, the

chain length distributions of both live and dead polymers are defined in terms of the weight density of the particle population with weighing the number of polymers on the number density of the particle population, the integral of which yields the total number of live or dead polymers of the particle population. An additional distribution is also defined, in the following way:

$g_n(i,V)$: discrete univariate live chain length number distribution function, giving the number of radicals of chain length n in a particle of size V, having i growing radicals.

From the relation between the different distributions described, the following properties can be easily deduced:

$$\int_0^\infty F(v)dV = \text{total number of particles (moles) per unit volume.}$$

$$\sum_{i=1}^{\infty} f_i(V) = F(V)$$

$$\sum_{n=1}^{\infty} \hat{f}_n(i,v) = i(v) f_i(V) = \left[\begin{array}{l}\text{number of growing}\\ \text{polymers in a particle}\\ \text{of vol. V}\end{array}\right] \cdot f_i(V)$$

$$\hat{f}_n(i,v) = g_n(i,v) \cdot f_i(V) = \left[\begin{array}{l}\text{number of dead}\\ \text{polymers in a particle}\\ \text{of vol. V}\end{array}\right] \cdot f_i(V)$$

$$\sum_{n=1}^{\infty} g_n(i,v) = i(V)$$

Dimensionless model equations

The following dimensionless variables have been defined:

$$\bar{V} = \frac{V}{V_o}$$

$$\bar{F}(\bar{v}) = \frac{F(v)}{F_o} \cdot V_o$$

$$\bar{t} = \frac{t}{t_o} \qquad t_o = \frac{V_o}{r_o}$$

$$[\bar{R}] = \frac{[R]}{[I]_o}$$

$$[\bar{T}] = \frac{[T]}{[I]_o} \tag{16}$$

$$[\bar{RM}] = \frac{[RM]}{[I]_o}$$

Total particle size distribution

$$\frac{\partial F(v,t)}{\partial t} + \frac{\partial}{\partial V}\left[\bar{r}_v F(v)\right] =$$

$$= \frac{1}{2}\int_{V_o}^{V} K_c\, e^{-E/RT}\,(V-v)^{-\frac{1}{3}}\,(v)^{-\frac{1}{3}}\,F(V-v)\,F(v)\,dv -$$

$$-F(V)\int_{V_o}^{\infty} K_c\, e^{-E/RT}\,(V\cdot v)^{-\frac{1}{3}}\,F(v)\,dv + k_a \bar{n}\,[R]_L\,\delta(V-V_o)$$

Radical number distribution

$$\frac{\partial}{\partial t} f_i(V,t) + \frac{\partial}{\partial V}\left[\bar{r}_V f_i(V,t)\right] = 2 f K_i [I]_p N_a V (f_{i-2} - f_i) +$$

$$+ \frac{K_3 + K_3'}{2} \frac{1}{N_a V}\left[(i+2)(i+1) f_{i+2} - i(i-1) f_i\right] +$$

$$+ \frac{1}{2}\int_{V_o}^{V} \sum_{j=1}^{i} K_c\, e^{-E/RT} (V-v)^{-\frac{1}{3}} (v)^{-\frac{1}{3}} f_j(V-v) f_{i-j}(v)\, dv -$$

$$- f_i(V,t)\int_{V_o}^{\infty} K_c\, e^{-E/RT} (v)^{-\frac{1}{3}} (v)^{-\frac{1}{3}} F(v)\, dv +$$

$$+ K_a \bar{n} [R]_L \delta(V - V_o)\delta_{ic} + K_4 [M]_p [f_{i+1} - f_i] +$$

$$+ K_5 [MR]_p [f_{i+1} - f_i] + K_{1a} [M]_p [MR]_p (N_a V)[f_{i-1} - f_i] +$$

$$+ K_8 [T][MR](N_a V)[f_{i-1} - f_i]$$

Growing polymer chain length distribution

$$\frac{\partial}{\partial t}\hat{f}_n(i,v,t) + \frac{\partial}{\partial v}\left[r_v \hat{f}_n\right] = 2f k_1 N_a V [I]_p \cdot [\hat{f}_n(i-2,v,t) -$$

$$\hat{f}_n(i,v,t)] + 2f k_1 N_a V [I]_p [f_{i-2}(v,t) - f_i(v,t)]\delta_{n1} +$$

$$+ k_2 [M]_p [\hat{f}_{n-1}(i,v,t) - \hat{f}_n(i,v,t)] +$$

$$+ \frac{k_3 + k_3'}{N_a V}\Big[(i+2)(i+1)\hat{f}_n(i+2,v,t) - i(i-1)\hat{f}_n(i,v,t) -$$

$$-(i+1)\hat{f}_n(i+2,v,t)] +$$

$$+ \int_{v_0}^{v} \sum_{j=0}^{i} k_c e^{-E/RT} (v-v)^{-\frac{1}{3}} (v)^{-\frac{1}{3}} \hat{f}_n(j,v-v) - f_{i-j}(v,t)dv -$$

$$- \hat{f}_n(i,v,t) \int_{v_0}^{\infty} k_c e^{-E/RT} (v\,v)^{-\frac{1}{3}} F(v)\,dv +$$

$$+ k_a \bar{n} [R]_L \delta(v-v_0)\delta_{n\bar{n}} - k_4 [M]_p \hat{f}_n(i,v,t) -$$

$$- k_5 [MR] \hat{f}_n(i,v,t) + k_7 [T]\left\{i f_i(v,t)\delta_{n1} - \hat{f}_n(i,v,t)\right\} +$$

$$+ k_{1a}[M][MR](N_aV)\left\{\hat{f}_n(i-1,v,t) - \hat{f}_n(i,V,t)\right\} +$$

$$+ k_{1a}[M][MR](N_aV) f_{i-1}(V,t)\,\delta n_2 +$$

$$+ k_8[T][MR](N_aV)\left\{f_{i-1}(V,t)\,\delta n_1 + \hat{f}_n(i-1,v,t) - \hat{f}_n(i,v,t)\right\}$$

Dead polymer chain length distribution

$$\frac{\partial}{\partial t} G_n(i,v,t) + \frac{\partial}{\partial V}\left[r_v G_n(i,v,t)\right] =$$

$$= 2f K_o [I]_p (N_a V)\left[G_n(i-2,v,t) - G_n(i,v,t) + \right.$$

$$+ \frac{K_3 + K_3'}{2N_a V}\left[(i+2)(i+1) G_n(i+2,v,t) - i(i-1) G_n(i,v,t)\right] +$$

$$+ \frac{K_3'}{2N_a V} f_{i+2}(v,t) \cdot g_n(i+2,v,t)(i+1) +$$

$$+ \frac{K_3}{2N_a V} f_{i+2}(v,t) \sum_{s=1}^{n-1} g_s(i+2,v,t)\, g_{n-s}(i+2,v,t) +$$

$$+ K_4 [M]_p \hat{f}_n(i,v,t) + K_5 [MR]_p f_n(i,v,t) +$$

$$+ \int_{v_o}^{v} \sum_{j=0}^{i} K_c e^{-E/RT} (v-v)^{-\frac{1}{3}} (v)^{-\frac{1}{3}} G_n(j, v-v, t) f_{i-j}(v,t)\, dv -$$

$$- G_n(i,v,t) \int_{0}^{\infty} K_c e^{-E/RT} (v \cdot v)^{-\frac{1}{3}} F(v)\, dv +$$

$$+ K_7 [T]_p \hat{f}_n(i,v,t) + K_8 [MR][T](N_a V) f_i(v,t)\, \delta n_1$$

When the set of equations is made dimensionless with the previously defined variables, the following groups appear:

$$C_1 = K_c V_o^{-\frac{2}{3}} F_o t_o$$

$$C_2 = K_a [I]_o \frac{t_o}{F_o}$$

$$C_3 = 2f K_1 [I]_o N_a V_o t_o$$

$$C_4 = \frac{1}{2}(K_3 + K_3') \frac{t_o}{N_a V_o}$$

$$C_5 = K_4 [I]_o t_o$$

$$C_6 = K_5 [I]_o t_o \qquad (18)$$

$$C_7 = K_{1a} [I]_o^2 N_a t_o V_o$$

$$C_8 = K_8 [I]_o t_o$$

$$C_9 = K_2 [I]_o t_o$$

$$C_{10} = K_7 [I]_o t_o$$

$$C_{11} = \frac{K_3'}{2} \frac{t_o}{N_a V_o}$$

$$C_{12} = \frac{K_3}{2} \frac{t_o}{N_a V_o}$$

Dimensionless particle size distribution

$$\frac{\partial}{\partial \bar{t}} \bar{F}(\bar{v},\bar{t}) + \frac{\partial}{\partial \bar{v}} [\, \bar{r}_v F(\bar{v}) \,] =$$

$$= \frac{1}{2} C_1 \int_{\bar{v}_0}^{\bar{v}} e^{-E/RT} (\bar{v}-\bar{v})^{-\frac{1}{3}} (\bar{v})^{-\frac{1}{3}} \bar{F}(\bar{v}-\bar{v}) \bar{F}(\bar{v}) d\bar{v} -$$

$$- C_1 \bar{F}(\bar{v}) \int_{\bar{v}_0}^{\infty} e^{-E/RT} (\bar{v})^{-\frac{1}{3}} (\bar{v})^{-\frac{1}{3}} F(\bar{v}) d\bar{v} + C_2 \bar{n}[\bar{R}]_l \bar{\delta}(\bar{v}-\bar{v}_0)$$

Dimensionless radical number distribution

$$\frac{\partial}{\partial \bar{t}} \bar{f}_i (\bar{v},\bar{t}) + \frac{\partial}{\partial \bar{v}} [\, \bar{r}_v \bar{f}_i(\bar{v},\bar{t}) \,] = C_3 [\bar{I}]_p \bar{V} [\bar{f}_{i-2} - \bar{f}_i] +$$

$$+ C_4 \left(\frac{1}{\bar{v}}\right) [(i+2)(i+1)\bar{f}_{i+2} - i(i-1)\bar{f}_i] +$$

$$+ \frac{1}{2} C_1 \int_{\bar{v}_0}^{\bar{v}} \sum_{j=0}^{i} e^{-E/RT} (\bar{v}-\bar{v})^{-\frac{1}{3}} (\bar{v})^{-\frac{1}{3}} \bar{f}_j(\bar{v}-\bar{v}) \bar{f}_{i-j}(\bar{v}) d\bar{v} -$$

$$- C_1 \bar{f}_i(\bar{v}) \int_{\bar{v}_0}^{\infty} e^{-E/RT} (\bar{v})^{-\frac{1}{3}} (\bar{v})^{-\frac{1}{3}} \bar{F}(\bar{v}) d\bar{v} +$$

$$+ C_2 \bar{n}[\bar{R}]_l \bar{\delta}(\bar{v}-\bar{v}_0) \delta_{ic} + C_5 [\bar{M}]_p (\bar{f}_{i+1} - \bar{f}_i) +$$

$$+ C_6 [\bar{MR}] (\bar{f}_{i+1} - \bar{f}_i) + C_7 [\bar{M}][\bar{MR}](\bar{v}) [\bar{f}_{i-1} - \bar{f}_i] +$$

$$+ C_8 [\bar{T}][\bar{MR}]_p (\bar{v}) [\bar{f}_{i-1} - \bar{f}_i]$$

Dimensionless growing chain length distribution

$$\frac{\partial}{\partial \bar{t}} \bar{\hat{f}}_n (i,\bar{v},\bar{t}) + \frac{\partial}{\partial \bar{v}} [\bar{r}_v \bar{\hat{f}}_n] = C_3 \bar{v} [\bar{I}]_p \left\{ \bar{\hat{f}}_n (i-2,\bar{v},\bar{t}) - \bar{\hat{f}}_n (i,\bar{v},\bar{t}) \right\} +$$

$$+ C_3 \bar{v} [\bar{I}]_p \left\{ \bar{f}_{i-2} (\bar{v},\bar{t}) - \bar{f}_i (\bar{v},\bar{t}) \right\} \delta_{n1} +$$

$$+ C_9 [\bar{M}]_p [\bar{\hat{f}}_{n-1} (i,\bar{v},\bar{t}) - \bar{\hat{f}}_n (i,\bar{v},\bar{t})] + C_4 \left(\frac{1}{\bar{v}}\right) [(i+2)(i+1)$$

$$\bar{\hat{f}}_n (i+2,\bar{v},\bar{t}) - i(i-1) \bar{\hat{f}}_n (i,\bar{v},\bar{t}) - (i+1) \bar{\hat{f}}_n (i+2,\bar{v},\bar{t})] +$$

$$+ C_1 \int_{\bar{v}_0}^{\bar{v}} \sum_{j=0}^{i} e^{-E/RT} (\bar{v}-\bar{v})^{-\frac{1}{3}} (\bar{v})^{-\frac{1}{3}} \bar{\hat{f}}_n (j,\bar{v}-\bar{v}) f_{i-j} (\bar{v}) d\bar{v} -$$

$$- C_1 \bar{\hat{f}}_n (i,\bar{v}) \int_{\bar{v}_0}^{\infty} e^{-E/RT} (\bar{v})^{-\frac{1}{3}} (\bar{v})^{-\frac{1}{3}} F(\bar{v}) d\bar{v} +$$

$$+ C_2 \bar{n} [\bar{R}]_L \bar{\delta} (\bar{v}-\bar{v}_0) \delta_{n\bar{n}} - C_5 [M] \bar{\hat{f}}_n (i,\bar{v}) - C_6 \bar{\hat{f}}_n (i,\bar{v}) [\bar{MR}] +$$

$$+ C_{10} [\bar{T}]_p \left\{ i \bar{f}_i (\bar{v}) \delta_{n1} - \bar{\hat{f}}_n (i,\bar{v}) \right\} +$$

$$+ C_7 [\bar{M}][\bar{MR}](\bar{v}) \left\{ \bar{\hat{f}}_n (i-1,\bar{v}) - \bar{\hat{f}}_n (i,\bar{v}) \right\} +$$

$$+ C_7 [\bar{M}][\bar{MR}](\bar{v}) \left\{ \bar{f}_{i-1} (\bar{v}) \right\} \delta_{n2} +$$

$$+ C_8 [\bar{T}][\bar{MR}]_p (\bar{v}) \left\{ \bar{f}_{i-1} (\bar{v}) \delta_{n1} + \bar{\hat{f}}_n (i-1,\bar{v}) - \bar{f}_n (i,\bar{v}) \right\}$$

Dimensionless dead polymer chain length distribution

$$\frac{\partial \bar{G}_n (i,\bar{v})}{\partial \bar{t}} + \frac{\partial}{\partial \bar{v}} \left[\bar{r}_v \bar{G}_n (i,\bar{v}) \right] =$$

$$= C_3 \bar{v} [\bar{I}]_p \left[\bar{G}_n (i-2,\bar{v},\bar{t}) - \bar{G}_n (i,\bar{v},\bar{t}) \right] +$$

$$+ C_4 \left(\frac{1}{\bar{v}}\right) \left[(i+2)(i+1) \bar{G}_n (i+2,\bar{v},\bar{t}) - i(i-1) \bar{G}_n (i,\bar{v}) \right] +$$

$$+ C_{11} \left(\frac{1}{\bar{v}}\right) \bar{f}_{i+2} (\bar{v}) g_n (i+2,\bar{v}) (i+1) +$$

$$+ C_1 \int_{\bar{V}_o}^{\bar{v}} e^{-E/RT} \sum_{j=0}^{i} (\bar{v}-\bar{v})^{-\frac{1}{3}} (\bar{v})^{-\frac{1}{3}} \bar{G}_n (j,\bar{v}-\bar{v}) f_{i-j} (\bar{v}) d\bar{v} -$$

$$- C_1 \bar{G}_n (i,\bar{v}) \int_{\bar{V}_o}^{\infty} e^{-E/RT} (\bar{v})^{-\frac{1}{3}} (\bar{v})^{-\frac{1}{3}} \bar{F}(\bar{v})\, d\bar{v} +$$

$$+C_{12}\left(\frac{1}{\bar{v}}\right) f_{i+2}(\bar{v})\left[\sum_{s=1}^{n-1} g_s(i+2,\bar{v},\bar{t})\, g_{n-s}(i+2,\bar{v})\right] +$$

$$+C_5[\bar{M}]_p \bar{\bar{f}}_n(i,\bar{v}) + C_6[\bar{M}\bar{R}]_p \bar{\bar{f}}_n(i,\bar{v}) +$$

$$+C_{10}[\bar{T}]_p \bar{\bar{f}}_n(i,\bar{v}) + C_8[\bar{M}\bar{R}]_p[\bar{T}]_p \bar{v} f_{i-1}(\bar{v})\delta_{n1}$$

3.4 Methods of solution

The multivariate dimensionless population balance equations described before, form a set of difference integro-differential equations which describe all possible particle sizes, radical numbers and chain length of the live and dead polymers.

Each equation is an infinite set in itself as the discrete variable (chain length and radical number) may range from one to infinity, and each equation belongs to another infinite set as the continuous variable (particle size) may be represented in terms of discrete grids ranging from zero to infinity. This aspect of the equations makes their solution intractable as they now stand.

For the continuous variable (particle size distribution) it is possible to prepare a characteristic function based on the definition of moments of order j according to:

$$\bar{\bar{F}}_v^{[j]} = \int_0^\infty (\bar{v})^j \bar{\bar{F}}(\bar{v})\, d\bar{v}$$

The analogous case for discrete distributions can be done by use of discrete transforms like Z transform or moment generating function.

The Z transform is defined as (58), (59):

$$\mathcal{Z} f(U) = \sum_{U=1}^{\infty} f(U) z^{-U} = \sum_{U=1}^{\infty} f(U)\, e^{\ln z^{-U}} = \sum_{U=1}^{\infty} f(U)\, e^{U \ln z^{-1}}$$

and permits the generation of moments of any order j for the distributions, based on the following property:

$$U^{[j]} = \sum_{U=1}^{\infty} U^{j} f(U) = \lim_{z \to 1} \frac{\partial^{j} \mathcal{Z}}{\partial (\ln z^{-1})}$$

Each set of infinite equations represented by each population balance, can be transformed (according to equation (24)) in one characteristic equation, from which all moments can be generated. In this case, we will end with four of these characteristic functions; one for the continuous distribution (sizes), and three for the remaining discrete distributions.

The total particle size distribution function F(V) is univariate in terms of particle volume V, and will produce univariate moments according to equation (23).

The radical number distribution function $f_i(V)$ is bivariate in terms of both the particle volume V, as a continuous variable and the radical number i as a discrete variable and the radical number i as a discrete variable; this yields bivariate moments as follows:

$$\bar{f}_{iv}^{[j,k]} = \int_0^\infty \sum_{i=0}^{\infty} (i)^j (\bar{v})^k f_i(\bar{v})\, d\bar{v}$$

The growing polymer chain length distribution function $f_n(i,V)$ and the dead polymer chain length distribution function $G_n(i,v)$ are trivariate, giving trivariate moments:

$$\bar{\hat{f}}_{ivn}^{[j,k,l]} = \int_0^\infty \sum_{i=0}^{\infty} \sum_{n=0}^{\infty} (i)^j (\bar{v})^k (n)^l \bar{\hat{f}}_n(i,\bar{v})\, d\bar{v}$$

$$G_{ivn}^{[j,k,l]} = \int_0^\infty \sum_{i=0}^{\infty} \sum_{n=0}^{\infty} (i)^j (\bar{v})^k (n)^l \bar{G}_n(i,\bar{v})\, d\bar{v}$$

Particularly, $G_{ivn}^{[o,o,j]}$ is of importance, as it provides the total amount of polymer formed at any time.

The aforementioned characteristic functions for the moment generation of any order j have been developed for the four population balances.

In the case of the discrete distributions, the moments of order J were also generated from the corresponding Z transformed equation.

The entire set of equations is included in Appendix A.

Focussing on this particular system, it is possible under certain assumptions, to uncouple the particle size distribution from the rest of the equations.

The coupling is given by the term on the left member (equation (19)), describing volume growth by chemical reaction of radicals

into the particles. As an approximation, it is possible either to introduce an average volume growth rate (r_v) based on total conversion, or entirely neglect the term, which is less relevant than that for particle growth by irreversible agglomeration.

On the basis of the previous approximation, three main possible approaches arise for the solution of the particle distribution, now as a single equation.

1) Discretization on both variables, volume and time: This method has been used for solving convolution equations in kinetic theory (Boltzmann equation) (62). Ray and Jain (63) attempted a solution for a particle size distribution with spontaneous particle generation, though several simplifications limit the validity of the model. The finite differences procedure becomes tedious when applied to convolutions.

2) Development of the moment equations: Once the characteristic function is prepared according to equation (23), it is possible to generate the moments of order 0,1,2,3,...N. If a solution is found for the N+1 equations of this system, the initial population balance can be expanded as a function of their moments. The particular functionality of the population balance will determine the number of moments required for an acceptable approximation (64). Sometimes, the resulting set of moment equations may present enclosure problems, when any moment becomes function of

moments of higher (or lower) order. For a system to be closed, those additional moments can be calculated as a function of integer moments (64). The derivation is based on the assumption that a given distribution can be represented analytically as a function of a set of moments. The method has been discussed in detail by Hulburt and Katz (64).

3) Method of weighed residuals: This method has been extensively used in the solution of population balance equations, as detailed in reference (67).

If we consider the solution of a scalar version of equation (15), results:

$$\frac{\partial W}{\partial t} + \frac{\partial}{\partial x}[\dot{x} W] = h(W,t) \qquad 0<X<\infty \quad t>0$$

$$W(x,0) = g(x) \qquad t = 0 \tag{25}$$

In the method of weighed residuals (MWR), the unknown distribution is expanded in terms of a finite number of trial functions $\{ n(x)\}$

$$W(x,t) = \sum_{n=1}^{N} C_n(t)\, \varphi_n(x)$$

$$W(x,0) = \sum_{n=1}^{N} C_n(0)\, \varphi_n(x) = g(x) \tag{26}$$

The $\{\varphi_n(x)\}$ may preferably come from a complete set in an appropriate space to which $W(x,t)$ belongs, i.e., $L_2(0,\infty)$ in this case.

The trial functions have also been assumed to be time independent although a more general formulation may eliminate this requirement.

The trial solution (26) is then substituted into equation (25) to obtain a residual function $R(x,t)$:

$$R(x,t) = L\left(\sum_{n=1}^{N} C_n(t)\,\varphi_n(x) - h\left(\sum_{n=1}^{N} C_n(t)\,\varphi_n(x), t\right)\right)$$

where L represents the continuity operator in the left hand side of equation (25). Also,

$$R(x,0) = \sum_{n=1}^{N} C_n(0)\,\varphi_n(x) - g(x)$$

The functions $\{C_n(t)\}$ together with their initial values $\{C_n(0)\}$ must be determined such that the residuals (27) and (28) are as close to zero as possible over the entire semi-infinite interval.

The essence of MWR is to accomplish this by orthogonalizing the residuals with a set of functions $\{\psi_n(x)\}$, also preferably from a complete set in $L_2[0,\infty)$. Thus,

$$\int_0^\infty R(x,t)\,\Psi_n(x)\,dx = 0$$

$$\int_0^\infty R(x,0)\,\Psi_n(x)\,dx = 0 \qquad n = 1,2,\ldots N \qquad (29)$$

Equations (29) will lead to a set of N ordinary differential equations in $C_n(t)$ where initial conditions can be obtained from (28). The success of the method rests on appropriate selection of the trial functions $\{\varphi_n(x)\}$ and the weighing functions $\{\psi_n(x)\}$. Singh et al. (65), (66) and Ramkrishna (67) have studied the effectiveness of different approximating functions in the solution of coagulation equations.

Melzak (44) obtained an analytical solution for the Brownian coagulation equation

$$\frac{dF(v,t)}{dt} = \frac{1}{2}\int_0^v F(v-v)\,F(v)\,dv - F(v)\int_0^\infty F(v)\,dv \qquad (30)$$

for initial distributions of the family of e^{-x}, and under some hypotheses previously used by Smoluchowsky (65) that limit the range of validity to small changes in particle size.

Singh and Ramkrishna (65) attempted numerical solutions of the same equation (30) by two different kinds of approximating functions:

1) Laguerre polynomials.

2) Problem specific polynomials, as defined by the authors. These are obtained by Gram-Schmidt orthogonalization of the set $\{x^n\}$ using an inner product weighted with a function that represents as closely as possible the true solution. In general, this weighting function is obtained by making different assumptions on our system equations that will permit to find an approximate analytical solution.

Comparison of both results with Melzak's analytical solution, shows that Laguerre polynomials require greater number of functions for poorer approximation, and only acceptable at short times. At longer times, this solution is either a poor approximation or becomes unstable. The use of problem specific polynomials leads to good results, but its applicability is restricted. It is not always possible to obtain the required approximate analytical solution through simplifications in the main system to solve.

With respect to the first possible method mentioned earlier, we have already pointed out the inconvenience of finite difference techniques for integro-differential equations with convolutions. Moreover, it becomes less encouraging to extend the method to the simultaneous solution of the population balances.

The second option, the method of the moments involves the simultaneous solution of a much larger number of coupled differential equations, as any initial population balance will be approximated in functions of its first j moments. Consequently, 4xj simultaneous equations have to be solved for the moments.

The complexity of the system and the large computation time expected, do not entirely justify the use of this technique.

As a conclusion, the method of weighted residuals seems more attractive, as it seems to be simpler and to involve less computation time.

A first trial was made on the particle size distribution, with the intention to extend its application to the simultaneous solution of the system.

When the equations for the weighted residuals described in a general sense (equation (29)) are applied to the particle size distribution (equation (19)), the following set of N non-linear ordinary differential equations is obtained:

$$\sum_{n=1}^{N} \frac{dC_n(t)}{dt} \int_0^{\infty} \varphi_n(v)\,\varphi_K(v)\,dv =$$

$$= A \int_0^{\infty} \varphi_K(v) \int_0^{v} \frac{1}{(v)^{\frac{1}{3}}} \cdot \frac{1}{(v-v)^{\frac{1}{3}}} \sum_{n=1}^{N} \sum_{m=1}^{N} C_n(t)\,C_m(t)\,\varphi_n(v)\,\varphi_m(v-v)\,dv\,dV -$$

$$- 2A \int_0^{\infty} \varphi_K(v) \sum_{n=1}^{N} \sum_{m=1}^{N} C_n C_m \frac{\varphi_n(v)}{(v)^{\frac{1}{3}}} \int_0^{\infty} \frac{\varphi_m(v)}{(v)^{\frac{1}{3}}}\,dv\,dV +$$

$$+ B \int_0^{\infty} \varphi_K(v)\,\bar{\delta}(v-v_0)\,dV \qquad (31)$$

$$(K = 1, 2, \ldots N)$$

where

$$A = K_c e^{-E/RT} (V_0)^{-\frac{2}{3}} (V_0)^{-\frac{2}{3}} F_0 t_0 = K'_c \Big|_{V=V_0} V_0^{-\frac{2}{3}} F_0 t_0$$

$$B = K_a [I]_0 \frac{t_0}{F_0}$$

$\varphi_n(V)$ = Laguerre polynomials (68)

$C_n(t)$ = time dependent coefficients (unknowns)

When the trial functions are chosen coincident with the weighting functions, the method is just that of Bubnov-Galerkin (69).

Attempts of an approximate analytical solution were also made. In addition to improve the understanding of what the real solution should be, the approximation can suggest more appropriate trial functions by Gram-Schmidt orthogonalization (65), (66).

Equation (19) has no analytical solution and admits no steady state assumptions because of the presence of the δ function. Smoluchowsky (65) demonstrated that at short times, it is possible to disregard the dependence of the agglomeration constant K_c upon the particle size. With this simplification and operating on that equation with the Laplace transform, the convolution integrals can be eliminated to give the much simpler result:

$$\frac{\partial \tilde{F}(s,t)}{\partial t} = A\tilde{F}^2(s,t) - 2A\tilde{F}(s,t) \cdot \left(\sqrt{\frac{B}{A}} \tanh \sqrt{AB}\, t\right) + B e^{-V_0 S}$$

With the transformation $2\frac{v'}{v} = \mathcal{F}$ $\alpha = \left(\frac{B}{4A}\right)^{\frac{1}{2}}$ $\tau = 2At$

and then $U(x) = v(t)$ with $X = \sinh \alpha t$, the following equation is obtained:

$$U''(1+X^2) + 2XU' + e^{-SV_o} U = 0 \qquad (32)$$

(Details of the derivation are given in Appendix B.)

No analytical solutions are known for this equation. In a last attempt to get an approximation, equation (32) was expanded in a power series of the form

$$U(x) = \sum_{n=0}^{\infty} A_n X^n$$

This procedure permits to obtain v(s,t) as

$$v(s,t) = A_1 \sum_{n=2}^{\infty} \prod_{K=2}^{n} \left[\frac{(2K-3)(2K-2) + e^{-SV_o}}{(2K-1)(2K-2)} \right] (-1)^{2n} \left[\sinh \sqrt{AB}\, t\right]^{2n-1}$$

which can be obtained in the volume domain by a term to term inversion. But the Laplace transform of the original particle size distribution

$$\mathcal{L}\, F(t) = \mathcal{F}(s,t) = \frac{2v'}{v}$$

does not present immediate analytical inversion. (Further details are given in Appendix B.)

C H A P T E R I V

COMPUTATIONAL TECHNIQUES

4.1 Conversion Versus Time Equation

The most important numerical techniques selected for the solution of the system will be described, together with an evaluation of some of the results obtained.

The first numerical approach was done on equation (12), governing the variation of total monomer consumption with time.

The greatest difficulty facing us, is the lack of reliable kinetic data to describe conversion. This aspect was already discussed when comparing different contributions of values for rate constants. Only constants for initiation, propagation and transfer to monomer are available, with discrepancies between authors greater than one order of magnitude. The situation becomes more difficult for the rest of the proposed kinetic steps, since only one reliable source of data is available (Schindler et al. (21)).

In order to verify the model, the kinetic parameters were adjusted by non-linear regression, according to Levenberg-Marquardt's algorithm (70). An improved version of it is available as subroutine ZXSSQ of the IMSL library. Experimental polymerization data for comparison were obtained from Talamini et al. (11). The mentioned algorithm suffered several difficulties due to singularities present in the objective function.

Numerous trials were made, increasing and decreasing the number of experimental points chosen for adjustment. In all cases, four experimental curves were treated simultaneously, corresponding to four different concentrations of initiator (Figure 6).

In a first step the objective function F was prepared as differences between experimental and calculated reaction rates at each point (r and r^{exp} respectively):

$$F = \sum_i \left(r - r^{exp} \right)_i^2$$

In a second step and with much better results, the objective function contained not only slopes (r and r^{exp}), but conversions as well (C and C^{exp}):

$$F = \sum_i \left(r - r^{exp} \right)_i^2 + \sum_i \left(C - C^{exp} \right)_i^2$$

In this last case, calculation of rates and conversions according to the proposed model, implies to solve the differential equation (for four different initiator concentrations) each time that the Marquardt's algorithm requires a new value for trial.

The solution of the differential equation was obtained with the subroutine DVOGER from the IMSL library, which consists in an improved version of Gear's method (71). One of the options of the algorithm permits optimization of the integration step, which allows a considerable reduction of the computation time.

One of the best results was obtained by fixing:

$$k_1 = 1.82\text{x}10^{-6} \text{ sec}^{-1} \text{ (initiation)}$$

$$k_2 = 1.1\text{x}10^{4} \text{ l/mole-sec (propagation)}$$

$$k_4 = 9.35 \text{ l/mole-sec (transfer to monomer)}$$

$$k_{1a} = 100. \text{ l/mole-sec (reinitiation)}$$

The regression on the remaining two constants provides the following values:

$$k_a = 260. \text{ sec}^{-1} \text{ (agglomeration)}$$

$$k_3 = 4.13\text{x}10^{8} \text{ l/mole-sec (termination)}$$

A comparison of these results are given in Figure (6).

4.2 Particle size distribution

Regarding the solution of the particle size distribution function by the method of weighted residuals, it was already pointed out that the orthogonalization of the residuals according to equations (27), (28) and (29) led to a system of N ordinary non-linear differential equations (equation (31)).

Laguerre polynomials were chosen as approximating functions, defined as:

$$(-1)^n L_n^{(\alpha)}(x) = \sum_{m=0}^{n} (-1)^m \frac{\Gamma(\alpha + n + 1)}{m!\,(n-m)!\,\Gamma(\alpha + n - m + 1)} x^{n-m}$$

with orthogonality in $0,+\infty)$ with respect to a weighting function $e^{-x}x^{\alpha}$:

$$\int_0^{+\infty} e^{-x} x^{\alpha} L_n^{(\alpha)}(x) L_m^{(\alpha)}(x)\, dx = 0 \qquad n \neq m \;;\; \alpha > -1 \tag{68}$$

All the terms of the system of equations (31) contain integrals, which were numerically evaluated by Romberg's automatic integration method (72). The algorithm is available as subroutine DCADRE in the IMSL library, highly effective by its very low relative error, and capacity to overcome poles and other singularities in the integrand.

The particular case of the first term in the right member of equations (31) require the solution of double integrals, one of them being a convolution on the particle size. The integration interval was divided in twenty points and each of them was used as upper limit of the convolution integral. The function for the second integration is given by the product of the previous convolution and the weighting function φ_k, both evaluated at each point. As only discrete values over the twenty points are then available, this second integration has to be calculated by Gauss-Legendre quadrature. High precision coefficients and weights were obtained from reference (73).

The system of N ordinary non-linear differential equations for the time dependent coefficients Cn's can be written in matrix form as:

$$|A| \cdot |\dot{c}| = |P|$$

where

$$A_{ij} = \int_0^\infty \varphi_i \varphi_j \, dx$$

The derivatives $\dot{C}_j = \frac{dc}{dt}$; can easily be made explicit by suitable choice of the weighting function, recalling the orthogonality property of Laguerre polynomials with a weighting function e^{-x}:

$$\int_0^\infty \varphi_i \varphi_j \, e^{-x} \, dx = 0$$

which makes all the off-diagonal elements in A equal to zero.

However, a first trial showed that the approximation was not accurate enough. Because of the finite integration interval used, the A_{ij}'s were not zero but small positive and negative values.

The derivatives were then made explicit by inversion of the |A| matrix by means of subroutine LINV2F from IMSL library:

$$|\dot{c}| = |A|^{-1} \cdot |P|$$

The resulting stiff system of differential equations was solved by use of Gear's method (subroutine DVOGER of IMSL library).

The Bubnov-Galerkin's method did not provide satisfactory results in this particular case. All the solutions presented oscillations that are not meaningful to the proposed coagulation model.

This effect persisted when the number of approximating functions was changed from 5 to 8.

Several other trials were made by changing to the following approximating functions:

$$e^{-x} x^{\alpha} \qquad n = 1 \ldots N$$

$$x^{n} \qquad \alpha = 0,\ 0.5,\ 1.0,\ 2.0$$

In order to verify the effectiveness of the algorithm and programming, a simpler coagulation model was tried.

The previously mentioned equation (30) describes the agglomeration of a particulate system without spontaneous generation. The analytical solution has been performed for initial distributions of the family of e^{-x} (44), (65). Similar conditions to those described in last term were easily established in the program by suppressing the continuous particle generation.

The performance became satisfactory as the oscillations disappeared and good agreement was found between the analytical and numerical solution.

C H A P T E R V

CONCLUSIONS AND RECOMMENDATIONS FOR FURTHER WORK

The kinetic model

From the results obtained in the present study of a kinetic model, it has been possible to correlate conversion versus time over a wide range of initiator and chain transfer agent concentrations. But the available kinetic parameters were quite unreliable, as they exhibited big differences between different sources. Only a few experimental determinations are available, and possibly the first of them is that of Burnett and Wright (39). Latter contributors have systematically modified and adjusted the existing data to their particular problems, but no new significant contributions were found in the open literature. As the things stand now, it is imperative to experimentally verify the whole set of reaction rate constants.

The complexity of the kinetic scheme does not permit easy extraction of initiator decomposition rates and efficiencies from conversion versus time data data (dead chain and polymerization, and related plots). Spectroscopic methods EPR) may be useful in the determination of parameters for the initiation reaction. Verification of the rest of the kinetic steps, as well as the distribution of initiator between phases, should be attempted with the use of radiotracers.

Agitation conditions in the reaction medium is also an aspect that was given little attention. Dilatometric experiments are expected to be unreliable at very low conversions, and the reaction conditions, quite different from those in a well stirred autoclave. No experimental data have been found for PVC, relating the effect of mixing conditions on the overall kinetics. Only a few qualitative considerations on particle morphology and speed of agitation are available.

With regard to particle structure, simplified assumptions of uniform morphology, require to be validated by microscopy studies at different degrees of conversion.

The mathematical approach and the method of weighted residuals

The description of complex heterogeneous polymerization systems involve the solution of coupled population balance equations. The method of weighted residuals has shown its shortcomings, that are inherent to the method itself, and not to the particular functionality of a population balance. In the early stages of conversion, the expected solution to our problem is given by a very narrow distribution, as only monodisperse particles are spontaneously generated into the liquid phase.

The maximum number of approximating functions chosen was eight generalized Laguerre polynomials. Every time this number is changed, all the coefficients previously mentioned, have to be recalculated by numerical integration of simple and double integrals, the integrands being products of Laguerre polynomials. Obviously the

approximation with eight functions was poor, and presented oscillations in positive and negative values. The limitation is thus given in the excessive computational time involved.

Essentially, the trend of the solution has to be known a priori. This has been discussed in references (65) and (66) where "problem specific polynomials" are constructed by orthogonalization of a complete set of functions with an approximate solution to the problem, capable to perform its trend. The fact that the solution has to be known or approximated beforehand, was also emphasized by Villadsen and Michelsen (74). Their techniques are based on orthogonal collocation with modified Jacobi polynomials. These authors provide many examples, not necessarily population balances, which clearly demonstrate that wherever pronounced changes in slope occur, the amount of collocation points (or equivalently, approximating functions) has to be seriously increased in that region, i.e., by subdividing the interval and then matching the solutions with those from other intervals. Otherwise, the system will converge to a solution that may result totally irrelevant to the particular problem under study. The same has been verified in our case, where computational time limitations restrict the number of approximating functions and thus, the quality of the numerical solution. It is worth emphasizing once more, that these difficulties originate in the increased number of approximating functions required by the method of weighted residuals for a particular trend in the solution, and is not a characteristic of the functionality of the population balance itself.

From our preliminary results, the method of weighted residuals has not offered advantages compared to other techniques. Only a few heterogeneous polymerization systems could be successfully solved up to this date, and probably the best example to compare is the one described in reference (53). For this case of continuous emulsion polymerization, the discrete distributions may be simplified by neglecting the convolution terms. Expansion of the distributions as functions of their leading moments, and steady state assumptions, end in a system of agebraic equations of immediate solution. But these hypotheses are not valid for the bulk polymerization process. Many different time scales are present in the reactor, and stiffness problems arise when the number of approximating functions (or equations to solve) is increased beyond reasonable limits.

Further mathematical developments are required, in order to reduce the computing effort; otherwise, all the important information concerning molecular weight distributions cannot be obtained. The same is valid for any attempt to understand more complicated cases like multi-phase copolymerization and non-linear polymerization.

NOMENCLATURE

a	: particle diameter
c	: fractional conversion or concentration
D	: diffusion coefficient
d_m	: monomer density
d_p	: polymer density
E	: activation energy for coalesce, cal/mol
f	: initiator efficiency
$f_i(v,t)dv$	: number of particles containing i radicals in a volume v to v + dv at time t, moles/cm^3
$f_n(i,v,t)dv$	: number of radicals of chain length n in the number of particles (per unit volume) of size v to v + dv having i growing radicals, moles/cm^3
$F(v)dv$	: number of polymer particles of a volume v to v + dv, moles/cm^3
F_o	: a characteristic number of particles, moles.
$g_n(i,v,t)$	: number of radicals of chain length n in a particle of size V having i growing radicals, dimensionless.
$G_n(i,v,t)dv$	: number of dead polymers of chain length n in the number of particles (per unit volume) of size v to v + dv having i growing radicals, moles/cm^3
i	: number of radicals, dimensionless

$\bar{i}$: average number of radicals per particle, dimensionless

I : initiator, moles

I_o : initial initiator concentration, moles/cm^3

I_p : initiator concentration in particles, moles/cm^3

I_l : initiator concentration in liquid phase, moles/cm^3

k : Boltzmann constant

k_a : radical absorption rate constant, 1/sec

k_d : radical desorption rate constant, 1/sec

k_a : rate constant for radical precipitation in the liquid phase, 1/sec

$k_c(v,V,E)$: rate coefficient of coalescence between two particles of volume V and v, having an activation energy E

k_l : initiator decomposition rate constant, 1/sec

k_2 : propagation rate constant, 1/mol-sec

k_3 : termination rate constant, 1/mol-sec (disproportionation)

k_3' : termination rate constant, 1/mol-sec (coupling)

k_4 : transfer to monomer rate constant, 1/mol-sec

k_5 : termination rate constant of $R^\bullet$ with $MR^\bullet$, 1/mol-sec

k_6 : rate constant for self-termination of $MR^\bullet$, 1/mol-sec

Kla : reinitiation rate constant, 1/mol-sec

k_7 : rate constant for transfer to transfer agent, 1/mol-sec

k_8 : rate constant for chain promotion, 1/mol-sec

$[M]_o$: initial monomer concentration, mole/l

$[M]$: monomer concentration, mole/l

n : chain length of polymer, dimensionless

$\bar{n}$: average polymer chain length, dimensionless

N_A : Avogadro's number

P_0 : vapor pressure of pure component

Pm : monomer pressure

P_m^0 : equilibrium monomer pressure

r : radius of particle, variable

r_0 : a characteristic reaction rate, moles/l-sec

r_v : rate of particle growth, cm^3/sec

R : free radical

[R] : free radical concentration, moles/l

RM : radicals, product of degradative transfer

[RM] : MR radicals concentration, moles/l

T : chain transfer agent concentration

TR : radicals product of the transfer with transfer agent

[TR] : concentration of radicals, TR, mol/l

V : volume, main variable

ν : volume, subvariable

V_o : characteristic volume, (volume of precipitated oligomers

Superscripts

0 : pure component, or saturation conditions

Subscripts

p : in the polymer particles

l : in the liquid (monomer) phase

i : having i radicals

n : having a chain length n

Greek Symbols

$\delta(v-v_o)$: Delta function, 1 if $v-v_0$; 0 otherwise

η : dynamic viscosity

κ : inverse of the double layer thickness

ν : number of colliding particles per unit volume

ρ_{il} : number of radicals generated in the liquid phase, in moles

ρ_{ip} : number of radicals generated in the solid phase, ni moles

σ : surface tension

χ : interaction parameter (Flory-Huggins)

REFERENCES

1. J. C. Thomas, SPE J., 23 (10) 61(1967)
2. J. C. Thomas, Hydrocarbon Process., 47(11) 192(1968)
3. J. Boissel and N. Fischer, J. Macromol. Sci (Chem) A11(7), 1249(1977)
4. H. S. Mickley, A. S. Michaelis, and A. L. Moore, J. Polym. Sci. 60, 121(1962)
5. J. D. Cotman, M. F. Gonzalex and J. C. Claver, J. Polym. Sci. A1(5),1137(1967)
6. D. Bort, S. Kuchanov and V. Zegel'man, Vysokomol. Soyed. 12, 2742(1975)
7. R. Bengough and R. Norrish, Proc. Royal Soc.(London) A200, 301(1950)
8. J. Breitenbach and A. Schindler, J. Polym. Sci. 18, 435(1955)
9. M. Magat, J. Polym. Sci. 16, 491(1955)
10. G. Talamini, J. Polym. Sci. 4, 535(1966)
11. A. Crosatto Arnaldi, P. Gasparini and G. Talamini, Die Makromol. Chem. 117, 140(1968).
12. G. Talamini and G. Vidotto, Makromol. Chem. 53, 21(1962)
13. A. H. Abdel-Alim and A. E. Hamielec, J. Appl. Polym. Sci. 16, 783(1972)
14. J. Ugelstad, H. Lervik, B. Gardinovacki and E. Sund, Pure Appl. Chem. 25, 121(1971)

15. J. Ugelstad, H. Fløgstad, T. Hertzberg and E. Sund, Die Makromol. Chem. 164, 171(1973)

16. J. Ugelstad, J. Macromol. Sci. (Chem) A11(7), 1281(1977).

17. O. Olaj, Angew. Makromol. Chem. 47, 1(1975)

18. O. Olaj, J. Macromol. Sci. (Chem.) A11(7), 1307(1977)

19. O. Olaj, J. Macromol. Sci. (Chem.) A11(7), 1319(1977)

20. E. J. Arlman and W. Wagner, J. Polym. Sci. 9, 581(1951)

21. J. Breitenbach and A. Schindler, Die Makromol. Chem. 122, 51 (1969)

22. G. Vidotto, S. Brugnaro, and G. Talamini, Die Makromol. Chem. 140, 249(1971).

23. C. Bamford, W. Barb, A. Jenkins and P. Onyon, "Vinyl Polymerization by Radical Mechanisms," Academic Press.

24. A. Berens and V. Folt, Polymer Eng. Sci. 8, 5(1968)

25. J. Glass and W. Fields, J. Appl. Polym. Sci. 16, 2269(1972)

26. A. Berens, "Polymer Preprints" 15(2), 203(1974)

27. A. Berens, Angew. Makromol. Chem. 47, 97(1975)

28. A. Michaels , W. Vieth, and J. Barrie, J. Appl. Phys. 34, 1(1963)

29. Erling Sorvik, J. Polym. Sci. (Polym. Letters) 14, 735(1956)

30. Erling Sorvik and T. Hertzberg, J. Macromol. Sci. A11(7),1349 (1977)

31. M. George, R. Grisenthwaite, and R. Hunter, Chem. Ind. (London) 38,1114, (1958) 38, 1114(1958)

32. G. Boccato, A. Rigo, G. Talamini and F. Grandi, Makromol. Chem. 108, 218(1967)

33. A. Rigo, G. Palma, and G. Talamini, Makromol. Chem. 153, 219(1972)

34. K. Abbas, F. Bovey and F. Schilling, Makromol. Chem. Suppl. 1, 227(1975)

35. G. Park, J. Macromol. Sci. (Phys.) B14(1), 151(1977)

36. K. Abbas, J. Macromol. Sci. (Phys.) B14(1), 159(1977)

37. F. Danusso, Ric. Sci. Suppl.,25, 46(1955)

38. W. Atkinson, C. Bamford and G. Eastmond, Trans. Faraday Soc. 66, 1446(1970)

39. G. Burnett and W. Wright, Proc. Royal Soc., A221, 128(1954)

40. E. Farber and M. Koral, Polym. Eng. Sci. 8, 11(1968)

41. T. Uno and K. Koshida, Kobunshi 15, 824(1968)

42. A. Golovin, Bull. (Izv.) Acad. Sci. USSR Geophys. Series 5, 482(1963), 9, 880(1963); 10,1571(1963).

43. W. Scott, J. Atm. Sci. 25, 54(1968)

44. Z. Melzak, Quart. Appl. Math. 11, 231(1953)

45. "Colloid Science" Vol I, H. Kruyt Editor, Elsevier Pub. Co. (1952)

46. L. Barcalay, A. Harrington and R. H. Ottewill, Kolloid Z. u.Z. Polymere 250, 655(1972)

47. M. Von Smoluchowsky, Physik Z. 17,557(1916)

48. M. Von Smoluchowsky, Z. Physik. Chem. 92, 129(1917)

49. N. Fuchs, Z. Physik. 89, 736(1934)

50. R. J. Pugh and J. A. Kitchener, J. Colloid, Int. Sci. 35, 4(1971)

51. R. Hogg, T. Healy and D. Fuerstenau, Trans. Faraday Soc. 62, 1638(1966)

52. S. Usui, Progress in Surface and Membrane Science 5, 223(1972)

53. K. Min, dissertation, State University of New York at Buffalo (1976)

54. D. H. Napper and R. J. Hunter, Int. Rev. Sci. Ser. II 7, Chap. 3(1975)

55. R. Ottewill and T. Walker, Kolloid Z.Z. Polym. 227, 108(1968)

56. A. Bibeau and E. Matijevic- J. Colloid. Int. Sci. 43, 330(1973)

57. D. Ramkrishna, Chem. Eng. Sci. 26, 1134(1971)

58. W. Ray and R. L. Laurence, "Chemical Reactor Theory (A review)" Lapidus-Amundson editors, (Chap. 9).

59. W. H. Ray, J. Macromol. Sci. (Reviews) C8(1), 56(1972)

60. K. Min and W. Ray, J. Macromol. Sci. (Chem.) C11(2), 177(1974)

61. K. Min and W. Ray, J. Appl. Polym. Sci. 22, 89(1978)

62. T. Bramlette and R. Mallett, J. Fluid Mech. 42, 177(1970)

63. H. Ray and S. Jain, J. Polym. Sci. 19, 1297(1975)

64. H. Hulburt and S. Katz, Chem. Eng. Sci. 19, 555(1964)

65. P. Singh and D. Ramkrishna, J. Colloid. Int. Sci. 53, 214(1975)

66. P. Singh and D. Ramkrishna, Comp. and Chem. Eng. 1, 23(1977)

67. D. Ramkrishna, Chem Eng. Sci. 28, 1362(1973)

68. G. Sansone, "Orthogonal Functions" Interscience (1959)

69. S. Mikhlin, "Variational methods in Mathematical Physics," Pergamon Press (1964)

70. D. Marquardt, J. SIAM 11, 431(1963)

71. C. W. Gear, Math. Comp. 21, 146(1967)

72. Carl de Boor, "Mathematical Software," John Rice editor. Academic Press, 1971 (chapter 7).

73. A. Stroud and D. Secrest, "Gaussian Quadrature Formulas," Prentice Hall.

74. J. Villadsen and M. Michelsen, "Solution of Differential Equation Models by Polynomial Approximation" P. Hall 1978

75. E. Zichy, J. Macrom. Sci. (Chem) A11(7), 1205(1977)

LIST OF FIGURES

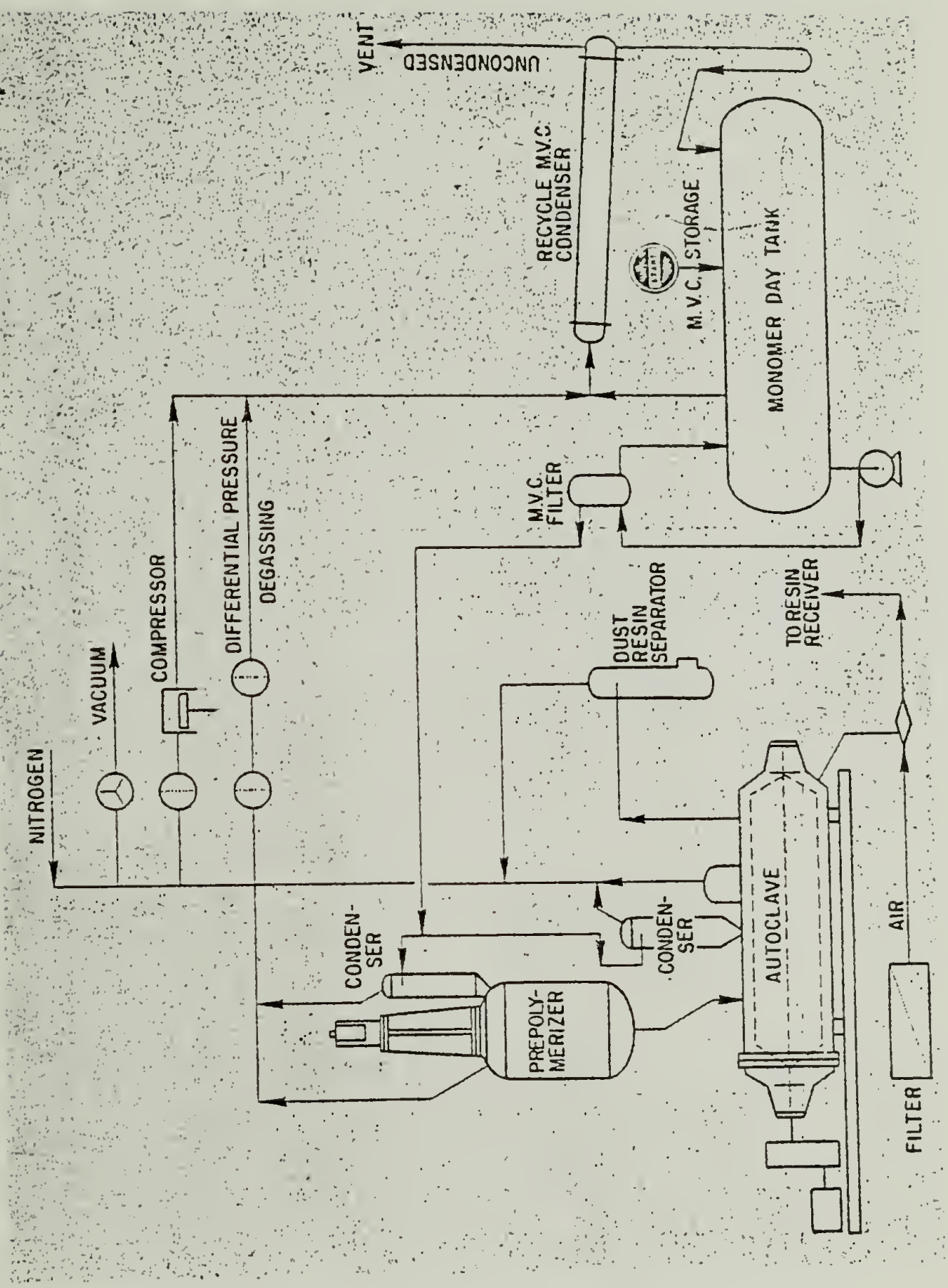

Fig. 1. Two-Step Bulk Polymerization Process.

(A) (B)

Fig. 2. Scanning electron micrograph, internal polymer morphology: (A) no additive, aggregates; (B) experimental stabilizer, spheres. (From reference 74.)

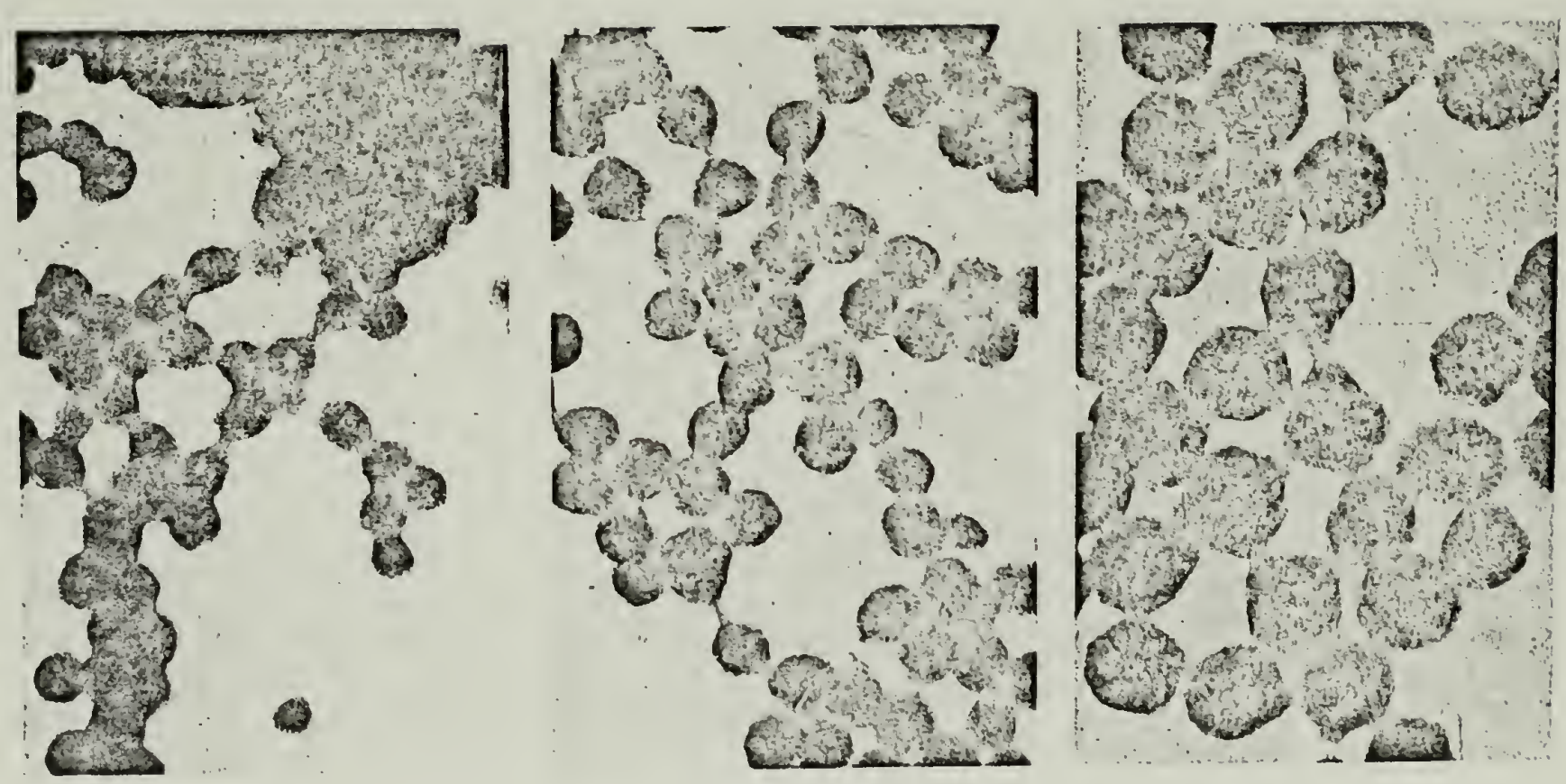

(a) (b) (c)

Fig. 3. Evolution of first formed particles during a polymerization run at 50°C (agitation 0.7 m/sec): (a) after 15 min (conversion 0.015%); (b) after 30 min (conversion 0.029%); (c) after 80 min (conversion 0.121%). x 50,000. (From Reference (3))

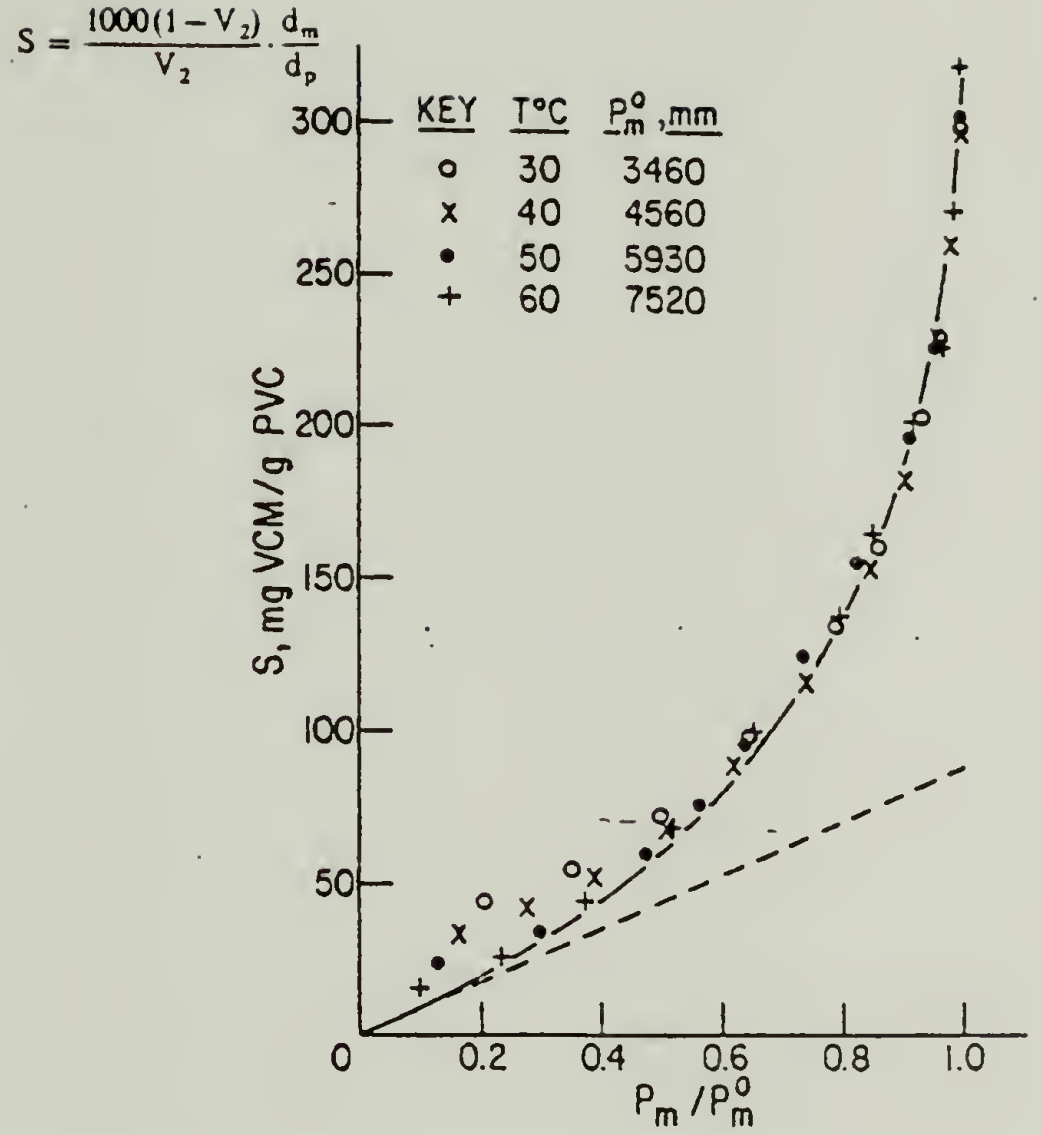

Fig. 4. VCM solubility, S, in PVC as a function of P_m/P_m^o points: experimental results from equilibrium vapor-pressure measurements; curve: calculated from equation (2) with χ = 0.98; broken line, equation (1) with k = 88 mg/g. (From reference (27)).

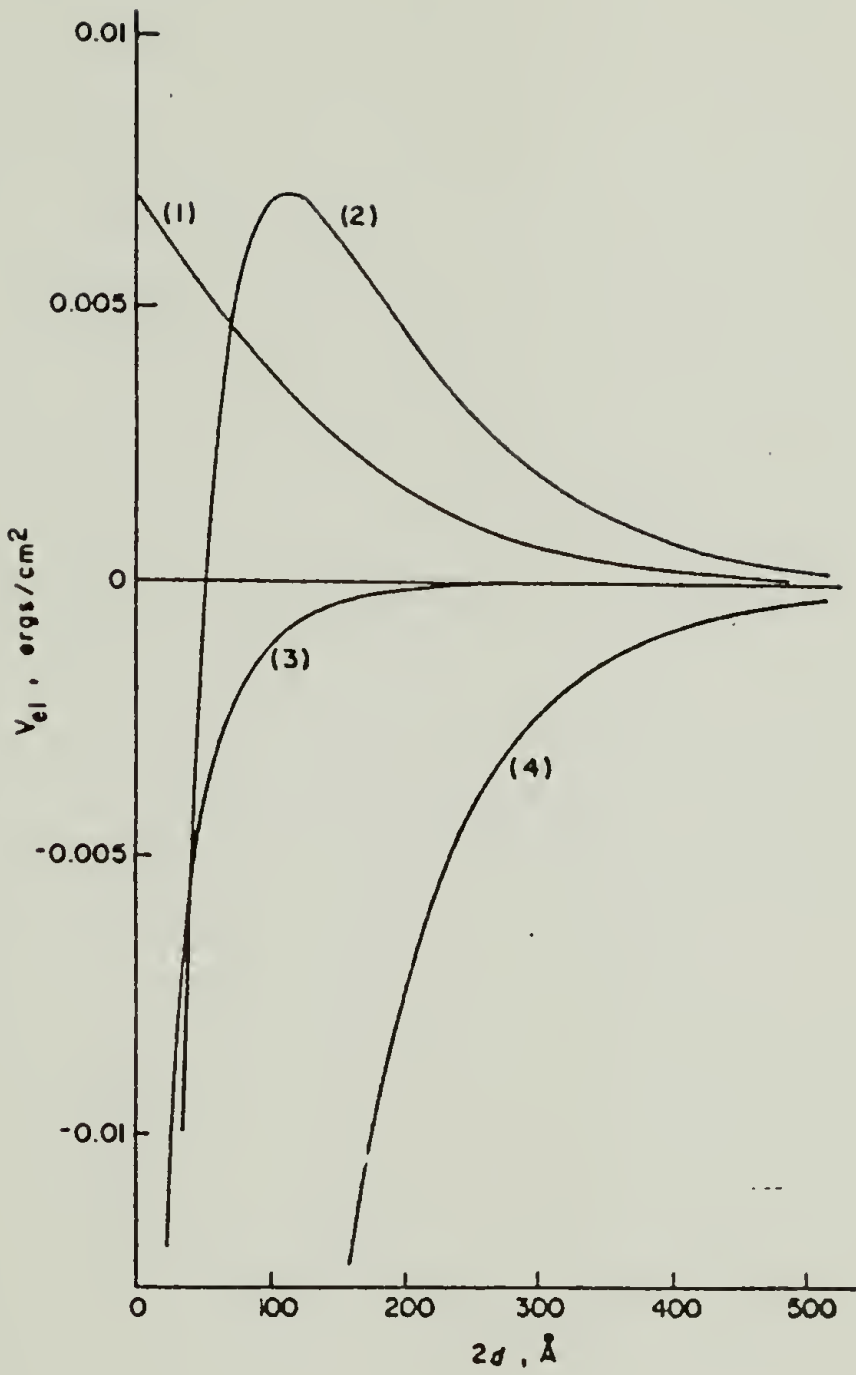

Fig. 5a. Potential energy of interaction between dissimilar double layers (V_{el}) as a function of the distance between particle surfaces (2d); c = 1 mM, 1-1 electrolyte (K = 10^6). (1) $\Psi_1 = \Psi_2 = 10$ mV; (2) Ψ_1 = 10mV, Ψ_2 = 30 mV; (3) Ψ_1 = 0 mV, Ψ_2 = 10 mV; (4) Ψ_1 = 10mV, Ψ_2 = -30 mV. (From reference (52)).

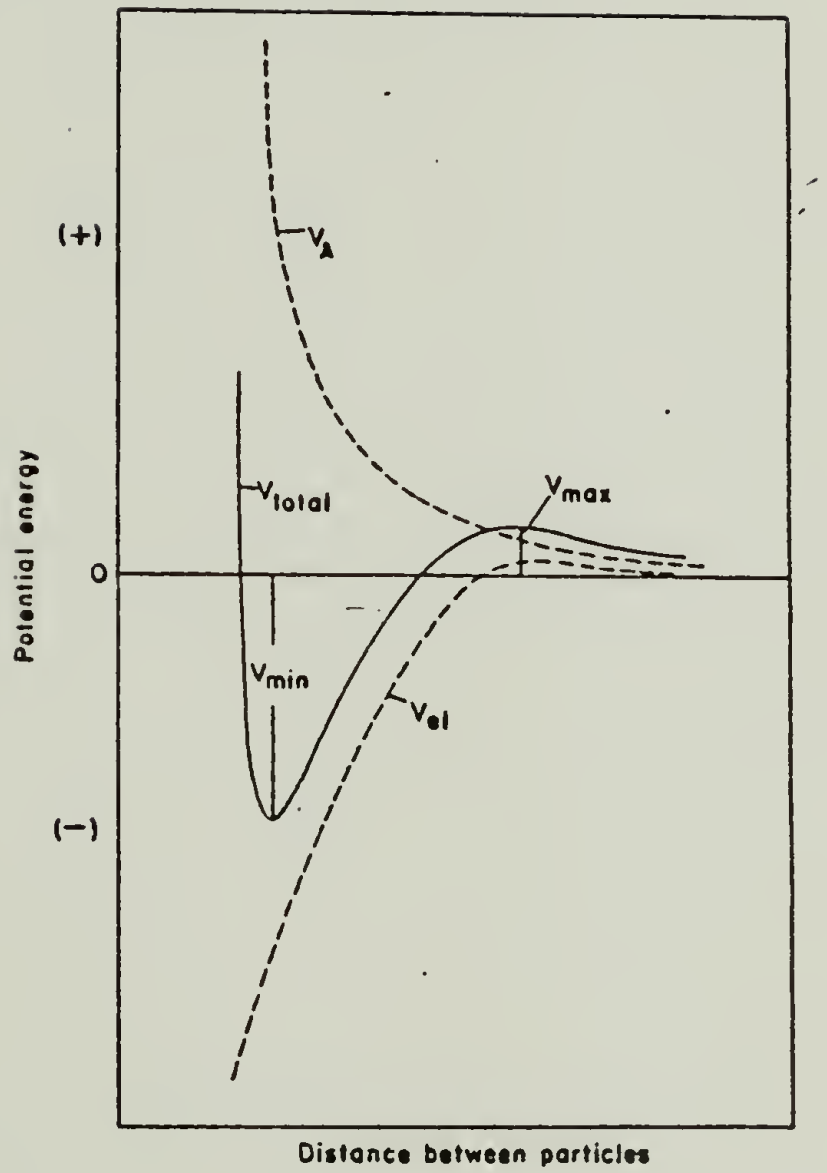

Fig. 5b. Schematic representation of total potential energy (V_{total}), electrical potential energy (V_{el}) of interaction, and van der Waals potential energy (V_A) between dissimilar particles as a function of the distance between particles, when
are of like sign.

(From reference (52)).

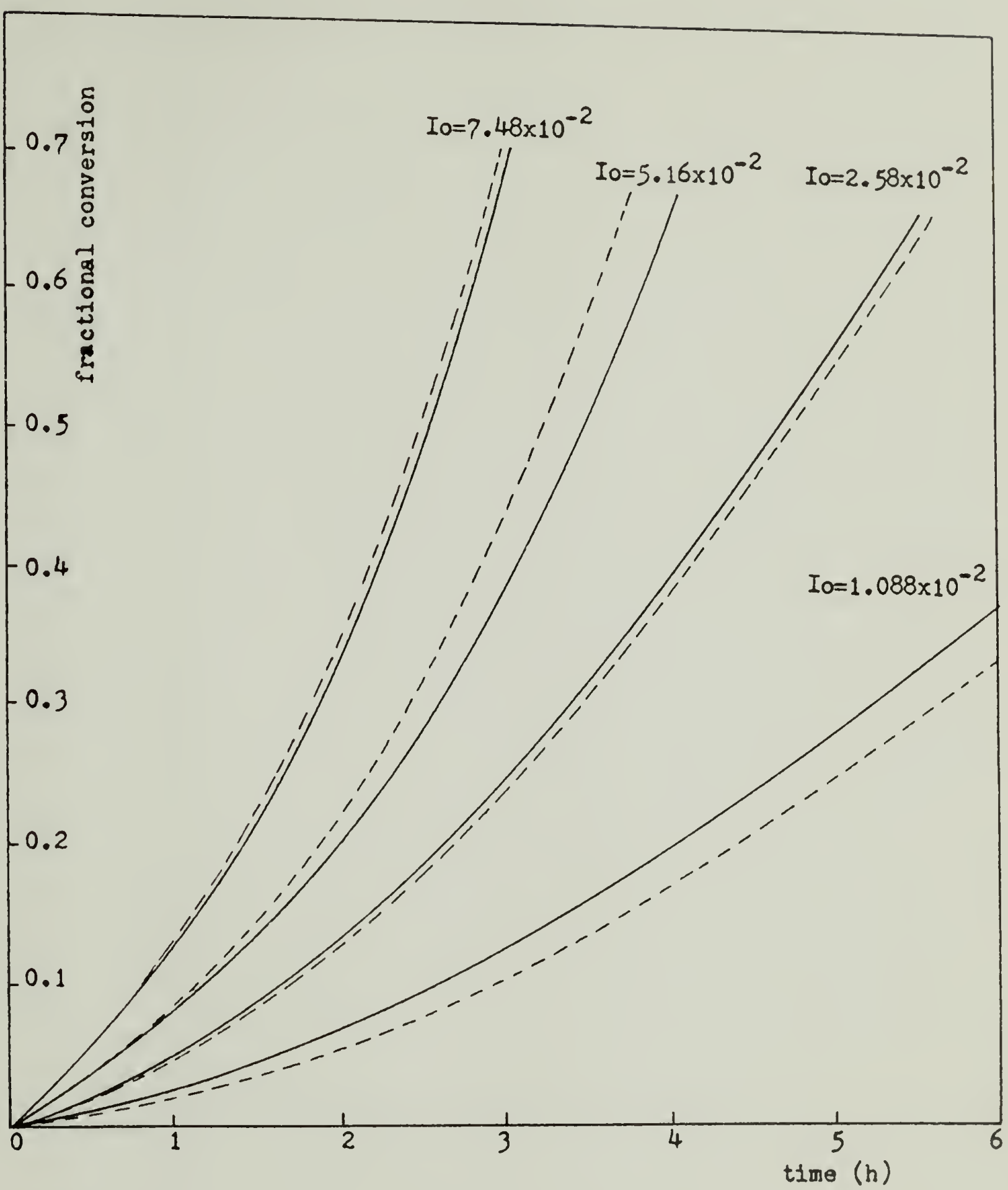

Fig. 6. Conversion versus time at four different initiator concentrations I_o (moles/liter).
(——) Experimental data from reference (11)
(----) Results from the model (equation (12))

APPENDIX A

Z TRANSFORMS AND MOMENT EQUATIONS

Moments of Order $\dot{j}$ for the Dimensionless Particle Size Distribution

$$\frac{\partial}{\partial \bar{t}} \bar{F}_v^{[j]} = j\, \bar{r}_v\, \bar{F}_v^{[j-1]} + \tfrac{1}{2} C_1 e^{-E/RT} \sum_{K=0}^{j} \binom{j}{K} \bar{F}_v^{[j-K-\frac{1}{3}]} \bar{F}_v^{[K-\frac{1}{3}]} -$$

$$- C_1 e^{-E/RT} \bar{F}_v^{[j-\frac{1}{3}]} \bar{F}_v^{[\frac{1}{3}]} + C_2 \bar{n} [\bar{R}]_L (\bar{V}_0)^j$$

Z Transform $\dot{j}$ for the Dimensionless Growing Polymer Chain Length Distribution

$$\frac{\partial}{\partial \bar{t}} \bar{\hat{f}}_z(i,\bar{v}) + \frac{\partial}{\partial \bar{v}} \left[\bar{r}_v \bar{\hat{f}}_z(i,\bar{v}) \right] = C_3 \bar{v} [\bar{I}]_p \left[\bar{\hat{f}}_z(i-2,\bar{v}) - \right.$$

$$\left. - \bar{\hat{f}}_z(i,\bar{v}) \right] + C_3 \bar{v} [\bar{I}]_p \cdot \left[\bar{f}_{i-2}(\bar{v}) - f_i(\bar{v}) \right] z^{-1} +$$

$$+ C_9 [\bar{M}]_p \left[\tfrac{1}{z} - 1 \right] \hat{f}_z(i,\bar{v}) + C_4 \left(\frac{1}{\bar{V}} \right) \left[(i+2)(i+1) \right.$$

$$\left. \bar{\hat{f}}_z(i+2,\bar{v},t) - i(i-1) \bar{\hat{f}}_z(i,\bar{v},\bar{t}) - (i+1) \bar{\hat{f}}_z(i+2,\bar{v},\bar{t}) \right] +$$

$$+ C_1 \int_{\bar{V}_0}^{\bar{v}} \sum_{j=0}^{i} e^{-E/RT} (\bar{v}-\bar{v})^{-\frac{1}{3}} (\bar{v})^{-\frac{1}{3}} \bar{\hat{f}}_z(j,\bar{v}-\bar{v}) f_{i-j}(\bar{v})\, d\bar{v} -$$

$$- C_1 \bar{\hat{f}}_z(i,\bar{v}) \int_{\bar{V}_0}^{\infty} e^{-E/RT} (\bar{v})^{-\frac{1}{3}} (\bar{v})^{-\frac{1}{3}} \bar{F}(\bar{v})\, d\bar{v} +$$

$$+ C_2 \bar{n} [\bar{R}]_L \bar{\delta}(\bar{V}_0 - \bar{V}_0) z^{-1} - C_5 [\bar{M}]_p \bar{\hat{f}}_z(i,\bar{v}) -$$

$$- C_6 [\bar{M}R]_p \bar{\bar{f}}_z(i,\bar{v}) + C_7 [\bar{M}][\bar{M}R](\bar{v}) \left\{ \bar{\bar{f}}_z(i-1,\bar{v}) - \right.$$

$$\left. - \bar{\bar{f}}_z(i,\bar{v}) \right\} + C_7 [M]_p [MR]_p (\bar{v}) f_{i-1}(\bar{v}) z^{-2} +$$

$$+ C_8 [\bar{T}]_p [\bar{M}R]_p (\bar{v}) \left\{ \bar{f}_{i-1}(\bar{v}) z^{-1} + \bar{\bar{f}}_z(i-1,\bar{v}) - \right.$$

$$\left. - \bar{\bar{f}}_z(i,\bar{v}) \right\}$$

Moments of Order K for the Dimensionless Growing Polymer Chain Length Distribution

$$\frac{\partial}{\partial \bar{t}} \bar{\bar{f}}_n^{[k]}(i,\bar{v}) + \frac{\partial}{\partial \bar{v}} \left[\bar{r}_v \bar{\bar{f}}_n^{[k]}(i,\bar{v}) \right] = C_3 \bar{v} [\bar{I}]_p \left\{ f_n^{[k]}(i-2,v) - \right.$$

$$\left. - \bar{\bar{f}}_n^{[k]}(i,\bar{v}) \right\} + C_3 \bar{v} [\bar{I}]_p \left\{ \bar{f}_{i-2}(\bar{v}) - \bar{f}_i(\bar{v}) \right\} +$$

$$+ C_9 [M] \left\{ \begin{array}{lll} k=0 & : & 0 \\ k=1 & : & \bar{\bar{f}}_n^{[0]} \\ k=2 & : & \bar{\bar{f}}_n^{[0]} + 2\bar{\bar{f}}_n^{[1]} \\ k=3 & & \bar{\bar{f}}_n^{[0]} + 3\bar{\bar{f}}_n^{[1]} + 3\bar{\bar{f}}_n^{[2]} \end{array} \right\} +$$

$$+ C_4 \left(\frac{1}{\bar{v}} \right) \left[(i+2)(i+1) \bar{\bar{f}}_n^{[k]}(i+2,\bar{v},\bar{t}) - i(i-1) \bar{\bar{f}}_n^{[k]}(i,\bar{v},\bar{t}) - \right.$$

$$-(i+1)\,\bar{\hat{f}}_n^{[K]}(i+2,\bar{V},\bar{t})\,] +$$

$$+C_1\int_{\bar{V}_0}^{\bar{V}}\sum_{j=0}^{i} e^{-E/RT}(\bar{V}-\bar{v})^{-\frac{1}{3}}(\bar{v})^{-\frac{1}{3}}\,\bar{\hat{f}}_n^{[K]}(j,\bar{V}-\bar{v})\,f_{i-j}(\bar{v})\,d\bar{v} -$$

$$-C_1\,\bar{\hat{f}}_n^{[K]}(i,\bar{v})\int_{V_0}^{\infty} e^{-E/RT}(\bar{V})^{-\frac{1}{3}}(\bar{v})^{-\frac{1}{3}}\,\bar{F}(\bar{v})\,d\bar{v} +$$

$$+C_2\,\bar{n}\,[\bar{R}]_L\,\delta(\bar{V}-\bar{V}_0) - C_5[\bar{M}]_p f_n^{[K]}(i,\bar{V}) -$$

$$-C_6[\bar{MR}]\,\bar{\hat{f}}_n^{[K]}(i,\bar{v}) + C_7[\bar{M}][\bar{MR}](\bar{V})\left\{f_n^{[K]}(i-1,\bar{V}) -\right.$$

$$\left.-f_n^{[K]}(i,\bar{V})\right\} + C_7[\bar{M}]_p[\bar{MR}]_p(\bar{V})f_{i-1}(\bar{V})\begin{Bmatrix} K=0 : 1 \\ K=1 : 2 \\ K=2 : 4 \\ K=3 : 8 \end{Bmatrix} +$$

$$+C_8[\bar{T}][\bar{MR}](\bar{V})\left\{f_{i-1}(\bar{V}) + \bar{\hat{f}}_n^{[K]}(i-1,\bar{V}) - \bar{\hat{f}}_n^{[K]}(i,\bar{V})\right\}$$

Z Transform of the Dimensionless Radical Number Distribution

$$\frac{\partial}{\partial\bar{t}}\bar{\bar{f}}(z,v) + \mu\frac{\partial}{\partial\bar{V}}\left[z\frac{dP}{dz}\bar{\bar{f}}(z,\bar{v})\right] = C_3[I]_p\bar{V}\left[\frac{1}{z^2}-1\right]\bar{\bar{f}}(z,\bar{v}) +$$

$$+C_4\left(\frac{1}{\bar{V}}\right)\left[(z^4-z^2)\frac{d}{dz^2}f(z,\bar{v}) + 2(z^3-z)\frac{dP}{dz}\bar{\bar{f}}(z,\bar{V})\right] +$$

$$+ \tfrac{1}{2} C_1 \int_{\bar{V}_0}^{\bar{V}} e^{-E/RT} (\bar{V}-\bar{v})^{-\frac{1}{3}} (v)^{-\frac{1}{3}} \bar{\bar{f}}(z,v)\, \bar{\bar{f}}(z,\bar{V}-\bar{v})\, d\bar{v} +$$

$$+ C_1 \bar{\bar{f}}(z,\bar{V}) \int_{\bar{V}_0}^{\infty} e^{-E/RT} (\bar{V})^{-\frac{1}{3}} (\bar{v})^{-\frac{1}{3}} F(\bar{v})\, d\bar{v} +$$

$$+ C_2 \bar{n} [\bar{R}]_L \bar{\delta}(\bar{V}-\bar{V}_0) z^{-1} + C_5 [\bar{M}]_p (z-1) \bar{\bar{f}}(z,\bar{V}) +$$

$$+ C_6 [\bar{M}\bar{R}]_p (z-1) \bar{\bar{f}}(z,\bar{V}) + C_7 [\bar{M}][\bar{M}\bar{R}]_p (\bar{V}) F(\bar{V}) \cdot$$

$$\left(\frac{1}{z}-1\right) \bar{\bar{f}}(z-\bar{V}) + C_8 [\bar{T}]_p [\bar{M}\bar{R}]_p (\bar{V}) \bar{F}(\bar{V}) \left(\frac{1}{z}-1\right) \bar{\bar{f}}(z,\bar{V})$$

Moments of Order K for the Dimensionless Radical Number Distribution

$$\frac{\partial}{\partial \bar{t}} \bar{f}^{[k]} + \mu \frac{\partial}{\partial \bar{V}} \bar{f}^{[k+1]} = C_3 [\bar{I}]_p \bar{V} \begin{cases} k=0 : 0 \\ k=1 : 2\bar{f}^{[0]} \\ k=2 : 4\bar{f}^{[0]} + 4\bar{f}^{[1]} \\ k=3 : 8\bar{f}^{[0]} + 12\bar{f}^{[1]} + 6\bar{f}^{[2]} \end{cases} +$$

$$+ C_4 \left(\frac{1}{\bar{V}}\right) \begin{cases} k=0 : 0 \\ k=1 : 2\bar{f}_1^{[1]} - 2\bar{f}^{[2]} \\ k=2 : -4\bar{f}^{[1]} + 8\bar{f}^{[2]} - 4\bar{f}^{[3]} \\ k=3 : 8\bar{f}^{[1]} - 20\bar{f}^{[2]} + 18\bar{f}^{[3]} - 6\bar{f}^{[4]} \end{cases} +$$

$$+ \tfrac{1}{2} C_1 \int_{V_0}^{V} e^{-E/RT} (V-\bar{v})^{-\frac{1}{3}} (\bar{v})^{-\frac{1}{3}} \begin{cases} K=0: & \bar{f}^{[0]}_{(\bar{v})} \bar{f}^{[0]}_{(\bar{V}-\bar{v})} \\ K=1: & f^{[1]}_{(\bar{v})} \cdot f^{[0]}_{(V-\bar{v})} + f^{[0]}_{(\bar{v})} f^{[1]}_{(V-\bar{v})} \\ K=2: & f^{[2]}_{(\bar{v})} f^{[0]}_{(\bar{V}-\bar{v})} + 2 f^{[1]}_{(\bar{v})} f^{[1]}_{(\bar{V}-\bar{v})} + \\ & + f^{[0]}_{(\bar{V})} \cdot f^{[2]}_{(\bar{V}-\bar{v})} \\ K=3: & \bar{f}^{[3]} \bar{f}^{[0]} + 3 \bar{f}^{[2]} \bar{f}^{[1]} + \\ & + 3 \bar{f}^{[1]} \bar{f}^{[2]} + \bar{f}^{[0]} \bar{f}^{[3]} \end{cases} d\bar{v}$$

$$+ C_1 \bar{f}^{[K]} \int_{\bar{V}_0}^{\infty} e^{-E/RT} (\bar{V})^{-\frac{1}{3}} (\bar{v})^{-\frac{1}{3}} \bar{F}(\bar{v})\, d\bar{v} \; +$$

$$+ C_2 \bar{n} [R]_L \bar{\delta}(\bar{V}-\bar{V}_0) + C_3 [M]_P \begin{cases} K=0: & 0 \\ K=1: & f^{[0]} \\ K=2: & f^{[0]} - 2f^{[1]} \\ K=3: & f^{[0]} - 3f^{[1]} - 3f^{[2]} \end{cases}$$

$$+ C_6 [MR]_P \begin{cases} K=0: & 0 \\ K=1: & f^{[0]} \\ K=2: & f^{[0]} - 2f^{[1]} \\ K=3: & f^{[0]} + 3f^{[1]} - 3f^{[2]} \end{cases} +$$

$$+ \Big[C_7 [M][MR](\bar{v}) F(\bar{v}) + C_8 [M][\bar{T}](\bar{V}) F(\bar{v}) \Big] \cdot \begin{cases} K=0: & 0 \\ K=1: & f^{[0]} \\ K=2: & f^{[0]} + 2f^{[1]} \\ K=3: & f^{[0]} + 3f^{[1]} + 3f^{[2]} \end{cases}$$

Z Transform of the Dimensionless Dead Polymer Chain Length Distribution

$$\frac{\partial}{\partial \bar{t}} \bar{G}_z(i,\bar{v}) + \frac{\partial}{\partial \bar{V}} \left[\bar{r}_v \bar{G}_z(i,\bar{v}) \right] = C_3 \bar{v} [\bar{I}]_p \left[\bar{G}_z(i-2,\bar{v}) - \bar{G}_z(i,\bar{v}) \right] + C_4 \left(\frac{1}{\bar{V}}\right) \left[(i+2)(i+1) \bar{G}_z(i+2,v) - i(i-1) \bar{G}_z(i,\bar{v}) \right] + C_{11} \left(\frac{1}{\bar{V}}\right) \bar{f}_{i+2}(\bar{v}) \bar{g}_z(i+2,\bar{v})(i+1) +$$

$$+ C_{12} \left(\frac{1}{\bar{V}}\right) f_{i+2}(\bar{v}) \left[\bar{g}_z(i+2,\bar{v}) \right]^2 +$$

$$+ C_1 \int_{\bar{V}_0}^{\bar{v}} \sum_{j=0}^{i} e^{-E/RT} (\bar{v}-\bar{v})^{-\frac{1}{3}} (\bar{v})^{-\frac{1}{3}} \bar{G}_z(j,\bar{v}-\bar{v}) f_{i-j}(\bar{v}) d\bar{v} -$$

$$- C_1 \bar{G}_z(i,\bar{v}) \int_{V_0}^{\infty} e^{-E/RT} (\bar{v})^{-\frac{1}{3}} (\bar{v})^{-\frac{1}{3}} F(\bar{v}) d\bar{v} +$$

$$+ C_5 [\bar{M}]_p \bar{\hat{f}}_z(i,\bar{v}) + C_6 [\bar{M}]_p \bar{\hat{f}}_z(i,\bar{v}) +$$

$$+ C_{10} [\bar{T}]_p \bar{\hat{f}}_z(i,\bar{v}) + C_8 [\bar{MR}]_p [T](\bar{V}) \bar{\hat{f}}_{i-1}(\bar{v}) z^{-1}.$$

Moments of Order j for the Dimensionless Polymer Chain Length Distribution

$$\frac{\partial}{\partial \bar{t}} \bar{G}_n^{[j]}(i,\bar{v}) + \frac{\partial}{\partial \bar{v}} \left[\bar{r}_v \bar{G}_n^{[j]}(i,\bar{v}) \right] =$$

$$= C_3(\bar{v}) [\bar{I}]_p \left[\bar{G}_n^{[j]}(i-2,\bar{v}) - \bar{G}_n^{[j]}(i,\bar{v}) \right] +$$

$$+ C_4\left(\frac{1}{\bar{v}}\right) \left[(i+2)(i+1) \bar{G}_n^{[j]}(i+2,\bar{v}) - i(i-1) \bar{G}_n^{[j]}(i,\bar{v}) \right] +$$

$$+ C_{11}\left(\frac{1}{\bar{v}}\right) \bar{f}_{i+2}(\bar{v}) g_n^{[j]}(i+2,\bar{v}) + C_{12}\left(\frac{1}{\bar{v}}\right) f_{i+2}(\bar{v}) \left[g_n^{[j]} \right]^2 +$$

$$+ C_1 \int_{\bar{V}_0}^{\bar{v}} \sum_{j=1}^{i} e^{-E/RT} (\bar{v}-\bar{v})^{-\frac{1}{3}} (v)^{-\frac{1}{3}} G_n^{[j]}(j,\bar{v},\bar{v}) \bar{f}_{i-j}(\bar{v}) d\bar{v} -$$

$$- C_1 G_n^{[j]}(i,\bar{v}) \int_{V_0}^{\infty} e^{-E/RT} (\bar{v})^{-\frac{1}{3}} (\bar{v})^{-\frac{1}{3}} F(\bar{v}) d\bar{v} +$$

$$+ C_5 [\bar{M}]_p \hat{\bar{f}}_n^{[j]}(i,V) + C_6 [\bar{MR}]_p \hat{\bar{f}}_n^{[j]}(i,V) +$$

$$+ C_{10} [\bar{T}]_p \hat{\bar{f}}_n^{[j]}(i,\bar{v}) + C_8 [\bar{MR}] [\bar{T}](\bar{V}) f_{i-1}(\bar{v}) .$$

Trivariate Moments (o, o, j for the Dimensionless Dead Polymer Chain Length Distribution

$$\frac{\partial}{\partial \bar{t}} G^{[0,0,j]}_{i,v,n} = C_{11} \int_{\bar{V}_0}^{\infty} \left(\frac{1}{\bar{V}}\right) \sum_{i=0}^{\infty} f_{i+2}(\bar{v})\, g_n^{[j]}(i+2,\bar{v})\, d\bar{V} +$$

$$+ C_{12} \int_{V_0}^{\infty} \left(\frac{1}{\bar{V}}\right) \sum_{i=0}^{\infty} \left\{ \begin{array}{ll} j=0 : & \left[\bar{g}_n^{[0]}(i+2,\bar{v})\right]^2 \\ j=1 : & 2\,\bar{g}_n^{[0]}(i+2,\bar{v})\,\bar{g}_n^{[0]}(i+2,\bar{v}) \\ j=2 : & 2\,\bar{g}_n^{[2]}(i+2,\bar{v})\,\bar{g}_n^{[0]}(i+2,v) + \\ j=3 : & +2\left[\bar{g}_n^{[1]}(i+2)\right]^2 + \\ & +2\bar{g}_n^{[3]}(i+2,\bar{v})\,\bar{g}_n^{[0]}(i+2,\bar{v}) + \\ & +6\,g_n^{[2]}(i+2,\bar{v})\,\bar{g}_n^{[1]}(i+2,\bar{v}) \end{array} \right\} f_{i+2}(\bar{v})\, d\bar{v} +$$

$$+ C_1 e^{-E/RT}\, \bar{G}_1^{[0,-\frac{1}{3},j]} \cdot \bar{F}_V^{[-\frac{1}{3}]} -$$

$$- C_1 \int_0^{\infty} \sum_{i=0}^{\infty} \bar{G}_n^{[j]}(i,\bar{v}) \int_{V_0}^{\infty} e^{-E/RT} (\bar{V})^{-\frac{1}{3}} (\bar{v})^{-\frac{1}{3}} \bar{F}(\bar{v})\, d\bar{v}\, d\bar{V} +$$

$$+ C_5 [\bar{M}]_P \int_{\bar{V}_0}^{\infty} \sum_{i=0}^{\infty} \hat{\bar{f}}_n^{[j]}(i,\bar{v})\, d\bar{V} + C_6 [MR] \int_{V_0}^{\infty} \sum_{i=0}^{\infty} f_n^{[j]}(i,\bar{v})\, d\bar{V} +$$

$$+ C_{10} [\bar{T}]_P \int_{V_0}^{\infty} \sum_{i=0}^{\infty} \hat{\bar{f}}_n^{[j]}(i,\bar{v})\, d\bar{v} + C_8 [\bar{MR}][\bar{T}] \int_{\bar{V}_0}^{\infty} \sum_{i=0}^{\infty} (\bar{V}) f_{i-1}(\bar{v})\, d\bar{V}$$

APPENDIX B

APPROXIMATE ANALYTICAL SOLUTIONS

recalling equation (19)

$$\frac{\partial \bar{F}}{\partial \bar{t}}(v,t) = \frac{1}{2} C_1 \int_{\bar{V}_0}^{\bar{V}} e^{-E/RT} (\bar{V} - \bar{v})^{-\frac{1}{3}} (\bar{v})^{-\frac{1}{3}} F(\bar{V}-\bar{v}) F(\bar{v}) d\bar{v} -$$

$$- C_1 \bar{F}(\bar{V}) \int_{\bar{V}_0}^{\infty} e^{-E/RT} (\bar{V})^{-\frac{1}{3}} (\bar{v})^{-\frac{1}{3}} F(\bar{v}) d\bar{v} \quad +$$

$$+ C_2 \bar{n} [\bar{R}] \bar{\int} (\bar{V} - \bar{V}_0)$$

and defining

$$A = \frac{1}{2} C_1 e^{-E/RT} = \frac{1}{2} K_c' V_0^{-\frac{2}{3}} F_0 \cdot t_0$$

$$B = C_2 = K_A [\bar{I}]_0 \frac{t_0}{F_0}$$

It is possible to get a much simpler equation under the assumption of a kernel function for coagulation independent of the particle sizes. The justification has been previously discussed in the text. Then, it is possible to write equation (19) as:

Applying the Laplace transform,

$$\frac{\partial}{\partial t}\mathcal{F}(s,t) = A\mathcal{F}^2(s,t) - 2A\mathcal{F}(s,t)\mathcal{F}(0,t) + Be^{-\bar{V}_0 s}$$

as

$$s \to 0$$

$$\mathcal{F}'(0) = A\mathcal{F}^2(0) - 2A\mathcal{F}^2(0) + B$$

$$\mathcal{F}'(0) = -A\mathcal{F}^2(0) + B$$

substituting $\frac{v'}{Av} = \mathcal{F}_0$,

$$v'' - AB v = 0$$

The solution is

$$\mathcal{F}_0 = \sqrt{\frac{B}{A}}\tanh\sqrt{AB}\,t$$

Then,

$$\frac{\partial}{\partial t}\mathcal{F}(s,t) = A\mathcal{F}^2(s,t) - 2A\mathcal{F}(s,t)\sqrt{\frac{B}{A}}\tanh\sqrt{AB}\,t + Be^{-\bar{V}_0 s}$$

Let $\alpha = \left(\frac{B}{4A}\right)^{\frac{1}{2}}$, $\tau = 2At$

$$\frac{\partial \mathcal{F}}{\partial \tau} = \frac{1}{2}\mathcal{F}^2 - \alpha \mathcal{F} \tanh \alpha\tau + 2\alpha^2 e^{-V_0 S}$$

Introducing

$$-2\frac{v'}{v} = \mathcal{F}, \qquad \mathcal{F}' + \frac{1}{2}\mathcal{F}^2 = -2\frac{v''}{v}$$

$$-2\frac{v''}{v} + \alpha\left(-2\frac{v'}{v}\right)\tanh \alpha\tau = 2\alpha^2 e^{-\bar{V}_0 S}$$

or

$$v'' + \alpha \tanh \alpha\tau + \alpha^2 e^{-\bar{V}_0 S} = 0$$

With the replacement

$$x = \sinh \alpha t$$

$$U(x) = v(t)$$

$$\frac{dv}{d\tau} = \frac{dU}{dx}\frac{dx}{d\tau} = \alpha U' \cosh \alpha\tau = U'\alpha\left(1+x^2\right)^{\frac{1}{2}}$$

$$\frac{d^2 v}{d\tau^2} = \frac{d^2 U}{dx^2}\left(\frac{dx}{d\tau}\right)^2 + \left(\frac{dU}{dx}\right)\frac{d^2 x}{d\tau^2}$$

$$= U''\alpha^2 \cosh^2 \alpha t + U'\alpha^2 \sinh \alpha t$$

$$= U''\alpha^2\left(1+x^2\right) + U'\alpha^2 x$$

Introducing these expressions in the differential equation and dividing by α^2, results that

$$\left(1+x^2\right)U'' + 2xU' + e^{-V_0 S}U = 0$$

No analytical solution is known for this equation. Making a power series expansion of the form

$$U = \sum_{n=0}^{\infty} A_n X^n$$

the following recursion formula for the coefficients results:

$$A_n = - \frac{\left[(n+2)(n-1) + q \right]}{n(n-1)} A_{n-2}$$

$$q = e^{-\bar{V}_0 S}$$

Taking on account the relation between U and V and after replacement, the function V can be expressed as

$$v(s,t) = A_1 \sum_{n=2}^{\infty} \prod_{k=2}^{n} \left[\frac{(2k-3)(2k-2) + e^{-\bar{V}_0 S}}{(2k-1)(2k-2)} \right] \times$$

$$\times (-1)^{2n} \left[\sinh \sqrt{AB}\, t \right]^{2n-1}$$

The function V(t) can be obtained by a term to term inversion, resulting in a combination of delta functions. However, in the original distribution

$$\mathcal{F}(s,t) = \frac{2v'(s,t)}{v(s,t)}$$

a straightforward analytical inversion is not possible.